HHS Public Access

Author manuscript

Cell Rep. Author manuscript; available in PMC 2019 August 02.

Published in final edited form as:

Cell Rep. 2019 May 07; 27(6): 1794–1808.e5. doi:10.1016/j.celrep.2019.04.032.

Remodeling of Interstrand Crosslink Proximal Replisomes Is Dependent on ATR, FANCM, and FANCD2

Jing Huang[1,9,*], **Jing Zhang**[2,9], **Marina A. Bellani**[2], **Durga Pokharel**[2], **Julia Gichimu**[2], **Ryan C. James**[2], **Himabindu Gali**[3], **Chen Ling**[6], **Zhijiang Yan**[8], **Dongyi Xu**[7], **Junjie Chen**[4], **Amom Ruhikanta Meetei**[5], **Lei Li**[4], **Weidong Wang**[6], **Michael M. Seidman**[2,10,*]

[1]Institute of Chemical Biology and Nanomedicine, State Key Laboratory of Chemo/Biosensing and Chemometrics, College of Biology, Hunan University, Changsha 410082, China

[2]Laboratory of Molecular Gerontology, National Institute on Aging, NIH, 251 Bayview Blvd., Baltimore, MD 21224, USA

[3]Department of Pharmacology & Experimental Therapeutics and Medicine, Boston University School of Medicine, 72 East Concord St., K-712D, Boston, MA 02118-2526

[4]Department Experimental Radiation Oncology, University of Texas MD Anderson Cancer Center, Houston, TX 77225-0334, USA

[5]Division of Experimental Hematology and Cancer Biology and Cancer & Blood Diseases Institute, Cincinnati Children's Hospital Medical Center, Cincinnati, OH 45229, USA

[6]Laboratory of Genetics and Genomics, National Institute on Aging, NIH, 251 Bayview Blvd., Baltimore, MD 21224, USA

[7]Peking University, Beijing 100871, China

[8]Institute of DNA Repair Diseases, School of Basic Medical Sciences, Wenzhou Medical University, Wenzhou, China

[9]These authors contributed equally

[10]Lead Contact

SUMMARY

Eukaryotic replisomes are driven by the mini chromosome maintenance (MCM [M]) helicase complex, an offset ring locked around the template for leading strand synthesis by CDC45 (C) and GINS (G) proteins. Although the CDC45 MCM GINS (CMG) structure implies that interstrand crosslinks (ICLs) are absolute blocks to replisomes, recent studies indicate that cells can restart

*Correspondence: huangjing16@hnu.edu.cn (J.H.), seidmanm@grc.nia.nih.gov (M.M.S.).

AUTHOR CONTRIBUTIONS

J.H., J.Z., J.G., R.C.J., H.G., and D.P. performed experiments; M.A.B., J.H., J.Z., and M.M.S. designed and performed experiments; J.C., Z.Y., C.L., L.L., D.X., and A.R.M. constructed cell lines used in experiments; W.W. and M.M.S. designed experiments; and W.W., M.A.B., and M.M.S. prepared the manuscript.

SUPPLEMENTAL INFORMATION

Supplemental Information can be found online at https://doi.org/10.1016/j.celrep.2019.04.032.

DECLARATION OF INTERESTS

The authors declare no competing interests.

DNA synthesis on the side of the ICL distal to the initial encounter. Here, we report that restart requires ATR and is promoted by FANCD2 and phosphorylated FANCM. Following introduction of genomic ICLs and dependent on ATR and FANCD2 but not on the Fanconi anemia core proteins or FAAP24, FANCM binds the replisome complex, with concomitant release of the GINS proteins. *In situ* analysis of replisomes proximal to ICLs confirms the ATR-dependent release of GINS proteins while CDC45 is retained on the remodeled replisome. The results demonstrate the plasticity of CMG composition in response to replication stress.

Graphical Abstract

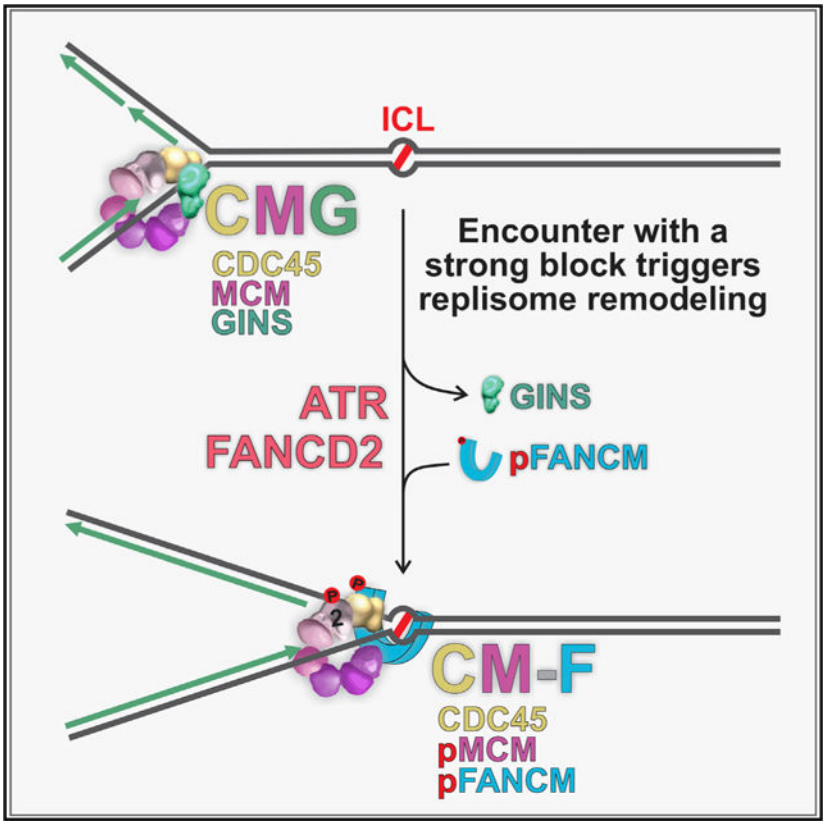

In Brief

Replication of the mammalian genome is driven by the replisome complex, which unwinds DNA and must overcome many impediments. Huang et al. find that the encounter of the CMG with a strong block triggers a change in replisome composition that is important for restart of replication past the obstruction.

INTRODUCTION

Replication stress is provoked by numerous impediments to the replisome, including covalent DNA lesions, DNA protein complexes, alternate DNA structures, breaks, and insufficient precursor nucleotides. Among the most potent blocks to replication are interstrand crosslinks (ICLs). They are formed by highly toxic cancer chemotherapy drugs

and DNA reactive compounds generated during normal cellular metabolism, including lipid peroxidation products (Niedernhofer et al., 2003), aldehydes (Pontel et al., 2015), and abasic sites (Price et al., 2017). ICLs are of additional interest because of the hyper-sensitivity to them of cells from patients with Fanconi anemia (FA). The FA proteins are involved in ICL repair, homologous recombination, mitochondrial function, and the regulation of inflammatory pathways (Brosh et al., 2017; Mamrak et al., 2017; Sumpter and Levine, 2017). The FA core complex ubiquitinates FANCD2 and FANCI, which contribute to ICL repair and genome stability pathways. Other FA proteins also support genome integrity. For example, the translocase FANCM (Meetei et al., 2005), although recently disqualified as a true FA protein (Bogliolo et al., 2018; Catucci et al., 2018), is important for resistance to replication stress and is implicated in DNA, including ICL, repair (Blackford et al., 2012; Kelsall et al., 2012; Pan et al., 2017; Wang et al., 2013).

ICLs are absolute blocks to unwinding of the double helix and, consequently, have always been considered absolute blocks to replication (Marmur and Grossman, 1961). This traditional view is consistent with the structure of the CDC45 MCM GINS (CMG) replisome. It is composed of the hetero-hexamer mini chromo-some maintenance (MCM) complex, which forms an offset ring that encircles duplex DNA when loaded in G_1 phase cells (Bochman and Schwacha, 2009; Li et al., 2015). The complexes are activated in S phase and, by a poorly understood conformational transition, are locked around the single-strand template for leading-strand synthesis by the binding of CDC45 and the GINS proteins (SLD5, PSF1, PSF2, and PSF3) (Costa et al., 2011; Georgescu et al., 2017; O'Donnell and Li, 2018; Yeeles et al., 2015). The closed structure implies that an ICL would block forward movement of the CMG. Although the composition and structure of the CMG have been the focus of intense biochemical research, the consequences of DNA damage to that structure *in vivo* have received much less attention.

The repair events that follow the encounter of replication forks with ICLs have been elucidated by the very influential work from the Walter laboratory (Knipscheer et al., 2012; Räschle et al., 2008). They report collisions of replication forks on both sides of an ICL carried on a plasmid replicating in a *Xenopus* egg extract. In their scheme, the structure formed by the dual fork collisions is the substrate for subsequent repair of the ICL (Zhang et al., 2015). CMG removal and fork remodeling allow access to repair enzymes, including the SLX4 nuclease platform, the XPF/ERCC1 incision endonuclease, and, for some ICLs, the NEIL3 glycosylase (Amunugama et al., 2018) (Fullbright et al., 2016; Klein Douwel et al., 2014; Long et al., 2014; Semlow et al., 2016; Yang et al., 2017).

The experimental system based on *Xenopus* egg extracts affords a detailed view of the molecular events following dual replication fork collisions with plasmid-borne ICLs. However, it does not address questions about replication in the vicinity of genomic ICLs in living mammalian cells, in which origins are widely separated. Thus, we developed an experimental strategy based on visualization of antigen-tagged ICLs in the vicinity of replication tracts on DNA fibers (Huang et al., 2013). As expected, we found evidence for both single- and double-fork collisions with ICLs. However, the most common pattern was consistent with the resumption of DNA synthesis on the distal side of the ICL, moving in the same direction as before the collision. Although unexpected, these observations have been

recently confirmed and extended by the Lopes group (Mutreja et al., 2018). We found that the translocase activity of FANCM was required for a major fraction of the “replication traverse” patterns (Figures 1A and 1B). Proteins shown to be partners of FANCM, such as MHF (Huang et al., 2013), BLM (Ling et al., 2016), and PCNA (Rohleder et al., 2016), were also important.

Although early, and more recent, data demonstrate the resilience of the replication machinery in the face of blocks (Rupp and Howard-Flanders, 1968; Yeeles and Marians, 2011; Taylor and Yeeles, 2018), it is challenging to reconcile the locked structure of the CMG with the high frequency of the traverse patterns. Consequently, we have examined the composition of replisomes proximal to ICLs during replication. We find that although CDC45 persists, there is a FANCM-, FANCD2-, and ATR-dependent absence of GINS proteins in ICL proximal replisomes.

RESULTS

Phosphorylation of FANCM by ATR Is Required for Replication Traverse of ICLs

Replication stress activates the ATR kinase, which phosphorylates FANCM and members of the MCM complex (Andreassen et al., 2004; Cortez et al., 2004; Matsuoka et al., 2007; Singh et al., 2013; Sobeck et al., 2009). We asked if knock down of ATR would influence replication fork encounters with ICLs. The results were striking; in the absence of ATR, traverse frequency was reduced to a few percent (Figure 1C). There was a corresponding increase in the frequency of stalled single forks, whereas dual fork collisions were unaffected. As expected, there was a small increase in the frequency of ICL encounters with forks resulting from the activation of dormant origins (Ge et al., 2007) (Figure 1A, iii). We obtained the same results when cells were exposed to an inhibitor of ATR, VE-821 (Figure S1A). ATR interacting protein (ATRIP) is an essential partner of ATR, and suppression of this protein also sharply reduced traverse frequency (Figure 1D).

ATR deficiency had no effect on the replication patterns in the vicinity of angelicin, a psoralen analog that forms only monoadducts (Figures 1E and S1B). These results clearly distinguished replication fork encounters with the trimethylpsoralen (TMP) adducts versus single-strand adducts. The implication that the ICLs were intact at the time of the fork encounter is supported by our observation of traverse patterns in cells deficient in the ERCC1/XPF ICL repair pathway (Huang et al., 2013) and the NEIL3 repair pathway (Semlow et al., 2016) (Figure S1C). Furthermore, although replication restart of the crosslinked template strands only takes a few minutes (Huang et al., 2013), un-hooking of the population of ICLs after replication fork collisions occurs over several hours (Figures S1D and S1E). Consequently, the restart patterns cannot be explained by replication past the single-strand remnant of an unhooked ICL.

FANCM is phosphorylated on multiple sites by ATR (Sobeck et al., 2009). Among them, serine 1045 phosphorylation has been shown to be important for recruitment to ICLs (Singh et al., 2013). We expressed FANCM or the phospho-resistant mutant of FANCM (S1045A) in *FANCM* knockout cells. The frequency of traverse in cells expressing the mutant FANCM was reduced to levels similar to those observed in FANCM-deficient cells (Figure 1F),

demonstrating that phosphorylation of FANCM on S1045 by ATR is required for FANCM's role in replication traverse of genomic ICLs.

The CDC7 kinase can phosphorylate MCM2 at some of the same sites as ATR (Charych et al., 2008), including at S108 (Figure S1F). We examined the relevance of this kinase on traverse frequencies by performing the assay in cells treated with CDC7-specific inhibitors PHA-767491 (Huang et al., 2013) or XL413 (Figure S1G). Neither inhibitor affected the pattern distribution. We concluded that ATR, not CDC7, was the key kinase controlling replication traverse.

FANCM Interacts with the MCM Complex

FANCM is known to associate with many proteins involved in various functions in support of genome stability (Blackford et al., 2012; Collis and Boulton, 2010; Deans and West, 2009; Gari et al., 2008). Given the importance of FANCM to replication restart past the ICLs, we asked if the list of interactors would extend to the MCM proteins. Cells were transfected with a plasmid encoding a FLAG-FANCM fusion protein, exposed to TMP/UVA and incubated for 1 h in the presence or absence of the ATR inhibitor VE821. Chromatin extracts were prepared and immunoprecipitated with an antibody against FLAG. The level of chromatin-associated FANCM was increased in the TMP/UVA-treated sample, consistent with previous reports (Kim et al., 2008). Western analysis of the immunoprecipitate demonstrated the presence of MCM2 and phosphorylated MCM2 (at S108) in the sample. MCM5, another member of the helicase complex, was also present. The appearance of these proteins in the immunoprecipitate (IP) was dependent on TMP/UVA and was abolished by incubation of the cells with the ATR inhibitor (Figure 2A). Treatment of the cell extracts with phosphatase prior to incubation with the antibody eliminated the MCM proteins in the IP. Thus, the association of the MCM proteins with FANCM required phosphorylation (Figure 2B).

To examine the interaction of FANCM and the MCM complex at the level of individual cells, we applied the proximity ligation assay (PLA), which reports the close association of proteins in cells (Söderberg et al., 2008). The PLA between MCM2 and FLAG-FANCM was performed in cells exposed to UVA only, cells exposed either to TMP/UVA, or TMP/UVA in the presence of the ATR inhibitor. The frequency of PLA signals in nuclei from UVA-only treated cells was quite low, was greatly increased by TMP/UVA treatment, and returned to control levels when the ATR inhibitor was included (Figures 2C and 2D). The same results were obtained with the endogenous FANCM as one of the partners of the PLA, indicating that the FLAG tag did not influence the behavior of FANCM (Figures S2A and S2B).

The Translocase Activity of FANCM Is Not Required for the MCM Interaction

The translocase activity of FANCM is ablated by the K117R mutation, which inactivates the ATPase (Meetei et al., 2005). In a coimmunoprecipitation (coIP) experiment, FLAG-FANCMK117R associated with the MCM proteins, including pMCM2S108, in an ATR-dependent manner, indicating that the translocase activity was not necessary for the interaction (Figure 2E). However, *FANCM* knockout cells expressing the K117R variant showed reduced traverse frequencies (Figure 2F). This result is consistent with our prior

report that cells expressing a different translocase mutant (FANCMD203A) had lowered traverse frequencies, comparable to those observed in FANCM knockout cells (Huang et al., 2013).

FANCM interacts with the FA core proteins, in support of FANCD2 monoubiquitylation (Xue et al., 2008). Previously, we found that the FA core proteins were not required for the traverse pathway (Huang et al., 2013). It was of interest to assess the relevance of FAAP24, another protein associated with FANCM, and the core complex. It is implicated in ICL repair and checkpoint responses (Ciccia et al., 2007; Collis et al., 2008; Horejŝí et al., 2009; Huang et al., 2010; Wang et al., 2013). However, the frequency of traverse patterns was not affected by knock down of FAAP24 (Figure S2C). These results indicated that the transactions engaged by FANCM/FAAP24 are distinct from the traverse pathway.

Altogether, these results demonstrate that in cells treated with TMP/UVA, ATR is required for the interaction of FANCM with the MCM proteins. Although the translocase activity of FANCM is important for the traverse patterns, it is not required for the association with the MCM complex.

The Association of FANCM with the MCM Proteins Is FANCD2 Dependent

FANCD2 and FANCI associate with the MCM proteins in a FA-core-protein-independent response to replication stress (Los-saint et al., 2013). Although our previous experiments showed that ubiquitination of FANCD2 was not required for traverse, they did not address a role for the non-ubiquitinated form (Huang et al., 2013). When we examined the replication patterns in PD20 cells with very little expression of FANCD2 (Figure 3A) but expression of FANCM similar to that in FANCD2 positive cells (Figure S3A), we found a reduction in traverse frequency, equivalent to that observed in FANCM-deficient cells. Similar results were obtained with HeLa cells with CRISPR/Cas9-mediated knock out of *FANCD2* (Figure S3B). The wild-type level of traverse events was restored in cells expressing the ubiquitination-resistant mutant form of FANCD2 (K561R) (Figure 3A), directly demonstrating the absence of a requirement for ubiquitination.

In order to examine the influence of FANCD2 on the association of FANCM and the MCM proteins, we expressed FLAG-FANCM in PD20 cells or PD20 cells complemented with wild-type FANCD2. In the coIP in PD20 cells, FLAG-FANCM failed to bring down the MCM proteins, whereas in the complemented cells they were recovered (Figure 3B). Similarly, the PLA between FLAG-FANCM and MCM2 was negative in the PD20 cells and positive in the complemented cells (Figures 3C and 3D). These experiments demonstrated that the association of FANCM with the MCM complex was dependent on FANCD2, as well as ATR (see below Figure 4G).

FANCD2 has been shown to bind the MCM complex following replication stress (Lossaint et al., 2013). The observation that FANCD2 was required for the interaction of FANCM and the MCM complex raised the possibility that FANCD2 and FANCM were associated with the same complex. To consider this, we exposed cells expressing FLAG FANCM to TMP/UVA, isolated chromatin, and performed IP against either the tagged FANCM or FANCD2. FANCM was present in the IP against FANCD2, whereas FANCD2 was present in the IP

against FLAG FANCM. This argued that FANCD2 and FANCM were on a complex defined by coIP (Figure 3E).

FANCI associates with FANCD2, and these two proteins have joint as well as distinct roles in response to replication stress (Castella et al., 2015; Sareen et al., 2012; Thompson et al., 2017). We asked if FANCI deficiency would influence the frequency of traverse patterns. The same decline in traverse frequency was observed with *FANCD2* and *FANCI* single knockout cells (confirming the results with PD20 cells). Similar results were obtained with *FANCD2*/*FANCI* double knockout cells, indicating that the influence of these proteins on traverse reflects involvement in a common pathway (Figure S3B).

FANCD2 interacts with and/or cooperates with multiple proteins in ICL repair and the response to replication stress. These include the homologous recombination (HR) proteins BRCA1/2 in the protection of stalled forks (Schlacher et al., 2012; Tacconi et al., 2017), the nuclease platform SLX4, and the incision nuclease ERCC1/XPF (Bhagwat et al., 2009; Klein Douwel et al., 2014; Yamamoto et al., 2011). We examined the influence of deficiencies in each of these genes on the frequency of traverse patterns. Traverse frequencies were unaffected by knock out of *ERCC1* (Huang et al., 2013), *BRCA2*, or *BRCA1* or knock down of *SLX4* (Figures S3C, S3D, and S3E). These results distinguished the role of FANCD2 in traverse from its functions in ICL repair and protection of nascent DNA at stalled forks.

Finally, we performed the traverse assay in cells in which the expression of both FANCM and FANCD2 was suppressed. There was no further reduction in traverse frequency in the double, relative to the single, knockdown cells (Figure 3F). We concluded that *FANCD2* and *FANCM* were epistatic with respect to their contribution to traverse of the ICLs.

The results of these experiments demonstrated the requirement of FANCD2 for the FANCM interaction with the MCM complex and explained the contribution of FANCD2 to the traverse patterns.

FANCM Association with MCM Proteins Is Coincident with the Release of GINS

We asked if treatment of cells with TMP/UVA would influence the composition of the CMG. After exposure to TMP/UVA, chromatin extracts were prepared and subjected to IP against MCM2 or pMCM2S108. FANCM, PSF1, and CDC45 appeared in the coIP against MCM2, the majority of which would not have encountered an ICL (the fiber analyses indicate that during the labeling period less than 10% of replication forks encounter an ICL). CDC45 was present when pMCM2S108 was the target of the IP. On the other hand, the GINS protein PSF1 was almost completely eliminated (Figure 4A). We repeated the analysis with FANCM as the target of the IP. pMCM2S108, MCM proteins, and CDC45 were recovered, but PSF1 was again absent (Figure 4B).

To determine the influence of the association of FANCM with the MCM complex on the components of the replisome, the coIP analysis was performed on chromatin proteins from *FANCM* knockout cells treated with TMP/UVA. The target of the IP was pMCM2S108. While CDC45 was in both samples, the GINS proteins were in the IP from *FANCM*$^{-/-}$

cells, but, as before, not in the IP from the *FANCM*$^{+/+}$ cells (Figure 4C). The interaction between FANCM and the GINS complex was further examined by PLA. Although both the wild-type and the translocase dead FANCM (K117R) were positive in the assay with pMCM2S108, neither were positive with PSF1 (Figures 4D, 4E, and 4F). The latter observation was further supported by an IP analysis with the translocase dead FLAG-KR117 variant of FANCM as the target. The MCM and CDC45 proteins were recovered but the GINS protein PSF1 was not (Figure S4A). Thus, the interaction of FANCM with the MCM proteins, regardless of translocase activity, was incompatible with the association of the GINS with the replisome.

Phosphorylation of FANCM Is Required for Association with the MCM Proteins

The requirement for phosphorylation of FANCM and the interaction with the MCM complex were examined by expressing the S1045A variant of FANCM in *FANCM* knockout cells and examining the composition of the MCM complex defined by pMCM2S108. PSF1 was not recovered in the IP against pMCM2S108 from cells expressing the wild-type FANCM. As expected, the wild-type FANCM was associated with the complex. However, in the IP from cells expressing FANCMS1045A, PSF1 was present, whereas the FANCM variant was not (Figure S4B). These results demonstrated the requirement for phosphorylation of FANCM at S1045 for the interaction with the MCM complex and the concomitant loss of the GINS proteins. We also performed PLA between FANCMS1045A and PSF1, pMCM2, and CDC45, with negative results (Figure S4C).

In the light of the requirement for FANCMS1045 phosphorylation, we examined the importance of phosphorylation of MCM2 on the ATR substrate site S108. A phospho-resistant variant of MCM2 (S108A) was expressed in cells in which the levels of wild-type MCM2 were suppressed by treatment with small interfering RNA (siRNA) (see Huang et al., 2013). Cells were exposed to Dig-TMP/UVA and the distribution of replication patterns determined. There was a reduction in traverse frequency (Figures S4D and S4E), although not as pronounced as in cells expressing FANCMS1045A (Figure 1F). This indicated that although phosphorylation of MCM2 on S108 contributed to replication restart past the ICL, it was not as important as phosphorylation on FANCMS1045. In keeping with these results, the PLA between FANCM and the MCM2S108A variant was readily detected although reduced compared to the PLA between the two wild-type proteins (Figure S4F).

The Release of the GINS Proteins Is Dependent on FANCD2

We also asked if FANCD2 would influence the composition of the CMG-containing pMCM2S108. *FANCD2* knockout cells or those cells expressing wild-type FANCD2 were exposed to TMP/UVA, chromatin was prepared, and IP was performed with pMCM2S108 as the target. FANCM was not recovered in the absence of FANCD2. However, consistent with the results with the *FANCM* knockout cells, both CDC45 and PSF1 were present in the IP from the *FANCD2* knockout cells (Figure 4G).

The results of all these experiments demonstrated that, following exposure of cells to TMP/UVA, there was a FANCM/FANCD2-dependent absence of GINS proteins from replisomes associating with FANCM. Phosphorylation of FANCM on S1045 was essential for the

interaction of FANCM with the MCM complex, while phosphorylation of MCM2 on S108 made a partial contribution to traverse frequencies and the interaction with FANCM.

ATR Regulates the Composition of ICL Proximal Replisomes

The preceding experiments could not show the proximity of proteins of interest and the ICLs. We addressed this by PLA between relevant proteins and the Dig tag on the ICLs. Cells were treated with UVA only, TMP/UVA, or Dig-TMP/UVA. After a 1-h incubation to allow replication forks to approach the ICLs, they were fixed and PLA between Dig and FANCM performed (Figures 5A and 5B). Positive signals were observed, whereas the controls (UVA only and TMP/UVA) were negative. However, as anticipated, we did not recover signals in the PLA between the Dig tag and the S1045 variant of FANCM, resistant to ATR phosphorylation (Figure S5A). The PLA between MCM2 and Dig was positive, and signal frequency increased in the absence of ATR activity (Figures 5C and 5D). These results were consistent with those of the fiber assays in which the frequency of stalled replisomes in the vicinity of ICLs was increased in the absence of ATR (Figure 1C). We also applied the PLA to the interaction between pMCM2S108 and the Dig tag. As expected, the signal was abolished by treatment with an ATR inhibitor (Figures 5E and 5D).

The PLA experiments could be interpreted as reflecting replication-dependent proximity of the CMG with ICLs. As an alternative explanation, we considered the possibility that the positive PLA between pMCM2 and the Dig tag represented an involvement of this protein in the DNA damage response to the ICL, unrelated to replication. As a test, we introduced laser localized ICLs (Muniandy et al., 2009) into nuclei of live cells and then scored for the appearance of pMCM2 in the ICL stripes (Figure S5B). For comparison, we also monitored the presence of a protein associated with the replisome, CAF1 (Gérard et al., 2006), which also participates in the DNA damage response (DDR) (Figure S5C). CAF1 was readily detected, but there was either no appearance of pMCM2 or, in a few cells, a barely detectable signal. These results argued against the positive PLA between the ICLs and pMCM2 as the result of a DDR-like recruitment of the MCM proteins.

In another test of the interpretation of the pMCM2S108: ICL PLA, we monitored the time course of the interactions. Previous experiments demonstrated that replication fork encounters with ICLs reached a plateau after about an hour following exposure to Dig-TMP/UVA (Huang et al., 2013). The pMCM2S108: ICL PLA showed similar plateau kinetics, consistent with the time course of replisome encounters (Figures 5F and 5G).

As an additional control experiment, we identified the cell cycle status of individual cells in the PLA between pMCM2S108 and the Dig-tagged ICLs by PCNA staining. Because there could be no replication fork collisions with an ICL in G_1 phase cells, these provided an assessment of non-specific-related signals. The results showed a strongly enhanced signal in S phase cells as compared to G_1 phase (Figures S5D and S5E).

The conclusion of these experiments was that during S phase there was an increase in the frequency of lesion proximal replisomes as a function of time after introduction of the ICLs. The frequency was further increased by inhibition of ATR, in agreement with an

accumulation of single forks stalled at ICLs in cells in which ATR activity was suppressed (Figures 1C and S1A).

The Release of GINS from ICL Proximal Replisomes Is Dependent on ATR and FANCM

The PLA analyses were extended to the interaction between CDC45 and the ICLs. Treatment of cells with the ATR inhibitor increased the signal frequency relative to untreated controls (Figures 6A and 6B). This, like the results with the MCM2: ICL PLA, was consistent with the presence of CDC45 on replisomes proximal to ICLs, the frequency of which was increased by inhibition of ATR.

We then examined the interaction of the GINS complex with the ICLs. The PLA between PSF1 and Dig was very low, in both G_1 and S phase cells (Figures S6A and S6B). However, consistent with the IP experiments (Figure 4C), the PLA between PSF1 and the ICLs rose in FANCM-deficient cells (Figures 6C and 6D). PLA between Dig and either CDC45 or PSF1 was performed in *FANCM* knockout cells expressing either wild-type FANCM or the K117R translocase inactive form. There was an increased Dig: CDC45 signal in the cells expressing K117R relative to those expressing the wild-type (Figures S6C and S6D). This was consistent with an accumulation, in the vicinity of ICLs, of replisomes associated with the FANCM K117R variant. On the other hand, there was no PLA between Dig and PSF in either the cells expressing the wild-type FANCM or the K117R version (Figures S6E and S6F).

Finally, we determined the influence of ATR inhibition on the PLA between the ICLs and three of the GINS proteins, namely, PSF1, PSF2, and PSF3. In control cells, the signals were very low but showed a striking enhancement in the presence of the ATR inhibitor (Figures 6E–6H). These results were in accord with the scenario in which the inhibition of ATR resulted in an increase, in the vicinity of ICLs, of replisomes that retained the GINS proteins.

DISCUSSION

ICLs were discovered several decades ago (Geiduschek, 1961; Marmur and Grossman, 1961) and ever since have been regarded as impassable blocks to any DNA pathway that requires unwinding. This perception would appear to be reinforced by the recent structural analyses of the eukaryotic replisome (Costa et al., 2011; Coster and Diffley, 2017; Li and O'Donnell, 2018; Zhai and Tye, 2017). Consequently, our observation of DNA synthesis proceeding in the same direction as a replication fork, but distal to the side of an ICL encountered by that replication fork, was unexpected in light of the topological constraints of the CMG. Thus, we addressed the possibility that the composition of the CMG complex might be modulated by proximity to an ICL. As we have previously shown the relevance of FANCM (Huang et al., 2013; Rohleder et al., 2016), it was of interest to ask if there was an association between it and the CMG complex. We found an interaction following exposure of the cells to TMP/UVA (it should be noted that this did not occur with exposure to UVA alone). The FANCM association with the MCM complex was dependent on FANCD2, which has been shown to bind MCM proteins after replication stress. This interaction is reduced by inhibition of ATR (Lossaint et al., 2013). Our observations are consistent with

those reported by the Constantinou group and argue that FANCD2 is important for the engagement of FANCM with the MCM proteins. This is functionally reflected in the decline in traverse frequency in FANCD2-deficient cells. On the other hand, FANCM associates with FAAP24 and FA core proteins, and neither of these complexes is relevant to the traverse patterns. Our results also indicate that FANCM is involved in two biochemically distinguishable events. Binding of the replisome, dependent on phosphorylation by ATR, does not require translocase activity. On the other hand, the contribution of FANCM to replication restart is dependent on phosphorylation and the translocase function.

We also found that the ATR-dependent interaction of FANCM with the CMG complex is accompanied by the continued association with CDC45 and the loss of the GINS proteins. This finding is reminiscent of that reported by the Costanzo group following the replication of chromatin in a *Xenopus* egg extract. They added S1 nuclease on the anticipation that single-strand regions on the template for the lagging strand would be cleaved. They demonstrated that RAD51 was required to maintain the integrity of the CMG complex. When RAD51 binding to the S1-treated chromatin was blocked, they observed the absence of the GINS proteins but the continued presence of CDC45 (Hashimoto et al., 2011). They speculated that the collapse of the fork was followed by the loss of the GINS, perhaps mediated by checkpoint kinases. Rebuilding of the fork by RAD51/HR would result in re-association of the GINS proteins, reconstructing the CMG complex. Our observations differ from those of Hashimoto et al., (2011) in that we found no requirement for HR functions BRCA1/2 for the traverse patterns. However, the loss of the GINS proteins under two quite different conditions of replication stress, in both live human cells and *Xenopus* egg extracts, suggests that this may be a common occurrence when the CMG encounters the numerous impediments that challenge successful replication of the genome. Furthermore, our observation of a FANCM: “CM” association implies a complexity of replisome composition, in response to blocks, that extends beyond the requirements for unchallenged replication. We note that our use of the PLA for assessing the proximity (or not) of proteins of interest to ICLs could be extended to any DNA modification or structure for which there are detection reagents (e.g., antibodies, binding proteins, and chemical tags).

A recent model of the CMG suggests that duplex DNA enters the complex, with separation of the lagging strand template occurring within the complex and extrusion of the single strand out the same port (Georgescu et al., 2017). If this model is correct, it has implications for the events following the encounter of a single fork with an ICL. Duplex DNA containing the ICL would enter the CMG and be recognized within the complex, presumably at the point at which strand separation was blocked. This might be the signal for activation of ATR, as it is unlikely that activation by lengthy stretches of single-strand DNA would be applicable in this scenario (Saldivar et al., 2017). Inducing the ATR cascade would promote the association of FANCM and the loss of the GINS proteins located on the surface of the CMG. Alternative models in which the duplex strands are separated before entry into the CMG are also compatible with this scheme (Abid Ali et al., 2016).

Traverse is not the only option available to a replisome stalled at an ICL. It might be persistently blocked, possibly because of an unfilled requirement for an additional factor, or an inactivating event that precludes restart of synthesis. The fork might reverse, replacing the

ICL in duplex DNA, perhaps allowing for repair by pathways unrelated to the replication fork (Williams et al., 2012; Zellweger et al., 2015; Amunugama et al., 2018; Mijic et al., 2017). A single stalled fork can be joined by another fork from the other side of the ICL, producing a dual fork collision. This would likely activate the ATR cascade again and trigger the repair pathway described by the Walter group (Räschle et al., 2008). The relative frequency of these choices will be a function of the concentrations or activity of relevant factors in the competition for the stalled fork and will vary in different cells under different conditions.

STAR★METHODS

CONTACT FOR REAGENT AND RESOURCE SHARING

Further information and requests for resources and reagents should be directed to and will be fulfilled by the Lead Contact, M. Seidman (seidmanm@grc.nia.nih.gov).

EXPERIMENTAL MODEL AND SUBJECT DETAILS

Mouse embryo fibroblast (MEF) NEIL $^{+/+}$ or $^{-/-}$ (sex unknown, embryos were not assessed for sex), MEF FANCM $^{+/+}$ or $^{-/-}$ (male), HeLa (female), CHO (female), 293T (female), and PD20 (male) cells were maintained in DMEM supplemented with 10% fetal calf serum, 100 U/mL penicillin, 100 μg/mL streptomycin sulfate. Chicken DT40 *FANCD2*$^{+/+}$ and *FANCD2*$^{-/-}$ (female) cells were grown in RPMI-1640 medium supplemented with 10% FBS, 1% chicken serum, in a 5% CO2 incubator at 39.5°C. *FANCD2*$^{-/-}$, *FANCI*$^{-/-}$. and *FANCD2*$^{-/-}$ *FANCI*$^{-/-}$, and *FANCM*$^{-/-}$ cells were prepared by CRISPR/Cas9 knockout of HeLa cells (female).

METHOD DETAILS

Co Immuno-Precipitation—For the FLAG tag pulldown experiments, 293T cells were transfected with plasmids expressing FLAG-tagged proteins using the PolyJet DNA Transfection Reagent (SignaGen Laboratories). Twenty four hours after transfection, the cells were incubated with or without 1mM TMP for 30 min prior to UVA irradiation (3 J/cm^2). In some experiments, cells were also incubated with 0.5μM ATR inhibitor VE-821. For the pulldown of endogenous phospho-MCM2S108, cells were treated with 1mM TMP/UVA. All the cells were incubated for another 1hr after UVA irradiation, and then harvested in cold PBS for chromatin extraction. To test the requirement for phosphorylation, extracts were incubated for 60 min at 37°C with 1 unit of calf intestine alkaline phosphatase per μg of protein in 100 mM NaCl, 50 mM Tris-HCl (pH 7.5), 10 mM $MgCl_2$, 1 mM dithiothreitol.

Chromatin extraction—10^7 cells were washed with PBS twice and suspended in buffer A (10 mM HEPES at pH 7.9, 10 mM KCl, 1.5 mM MgCl2, 0.34 M sucrose, 10% glycerol, 1 mM DTT, 10 mM NaF, 1 mM sodium orthovanadate, 0.1% Triton X-100, with protease and phosphatase inhibitors). Subsequently, the cells were placed on ice for 5 min. Cytoplasmic proteins were isolated from nuclei by low speed centrifugation (1300 × g for 4 min). The nuclear pellet was washed with buffer A and lysed in buffer B (3 mM EDTA, 0.2 mM EGTA, 1 mM DTT, protease and phosphatase inhibitors). The nuclei were left on ice for 10 min, and then centrifuged (1700 g for 4 min) to separate soluble nuclear proteins from

chromatin. Isolated chromatin was washed once with buffer B and centrifuged at high speed (10,000 g for 1 min) to remove the rest of the buffer. Chromatin was resuspended in benzonase buffer (20 mM Tris-HCl at pH 8.0, 0.2 mM $MgCl_2$, 2 mM NaCl, protease and phosphatase inhibitors) and benzonase (250 U/mL) was added and incubated at 4°C overnight, followed by another addition of benzonase and further incubation for 2 hr. Subsequently, the digested sample was clarified by centrifugation and the supernatant transferred to a new tube and adjusted to 200 mM NaCl, 50 mM Tris-HCl pH 7.4, 0.1% Tween 20, and protease and phosphatase inhibitors added.

For FLAG pulldown, the samples were incubated with anti-FLAG M2 Magnetic Beads (Sigma) at 4°C overnight by gentle inversion. For protein G beads, Dynabeads Protein G (Life Technologies) were incubated with anti pMCM2S108 or anti MCM2 or anti IgG antibodies for 30 min at room temperature. The antibody: bead complexes were captured with a magnet and washed three times with PBS-T. Dynabead-antibody complexes were suspended in the soluble chromatin protein solution and rotated overnight at 4°C. The beads were washed three times with 200 mM NaCl, 50 mM Tris-HCl pH 7.4, 0.1% Tween 20. The beads were resuspended in SDS-PAGE loading buffer. After heating for 10 min at 70°C, the proteins were analyzed by western blotting.

Western Blotting—The samples were lysed in NuPAGE Sample Buffer (Invitrogen), sonicated and boiled. Samples were resolved by 4%–12% Bis-Tris Protein Gels and blotted onto a PVDF membrane. Western blotting was performed according to standard procedures.

PLA assay—Cells were seeded in 35 mm glass bottom dishes (MatTek) and treated with or without 5 μM Dig-TMP, or 1 mM TMP. In some experiments cells were preincubated with the ATR inhibitor VE-821 (0.5 μM) for 30 min prior to UVA irradiation. In experiments with FLAG tagged proteins, cells were transfected with the appropriate plasmid with PolyJet DNA Transfection Reagent (SignaGen Laboratories). Twenty-four hours after transfection, the cells were treated with 5 μM Dig-TMP/UVA, incubated for 60 min at 37°C and then washed once with cold PBS and twice for 5 min in CSK buffer (10 mM PIPES, pH 7.0, 100 mM NaCl, 300 mM sucrose, 3 mM $MgCl_2$, 0.5% Triton X-100). Cells were then washed with cold PBS and fixed with 2% formaldehyde for 10 min at room temperature. After a PBS wash, they were incubated with −20°C methanol for 20 min. After washing with PBS they were treated with RNase (100 μg/ml) for 30 min at 37°C. Following another PBS wash the cells were incubated with the blocking buffer in the Duolink kit and the manufacturer's instructions were followed through the amplification step. The primary antibodies were mouse anti MCM2 (1/200), rabbit anti MCM2S108 (1/200), rabbit anti PSF1, rabbit anti PSF2, rabbit anti PSF3 (1/200), mouse anti digoxigenin (1/200), mouse anti PCNA (1/200), rabbit anti FANCM (1/200), mouse anti-FLAG (1/200) or rabbit anti-FLAG (1/200) (See Key Resources Table). To allow visualization of the individual target proteins, after amplification, the cells were incubated with goat anti rabbit Alexa Fluor 488 conjugate (1/1000) and goat anti mouse Alexa Fluor 568 conjugate (1/1000) for 45 min. After washing with PBS the plates were mounted in mounting medium containing DAPI (ProlongGold, Invitrogen). Specificity was confirmed by omitting one or the other primary antibody.

Imaging was performed on a Zeiss Axiovert 200 Microscope, and image analysis with the Axio Vision software packages (Zeiss).

DNA Spreading—Cells were incubated at 37°C for 1 hr with 5 μM Dig-TMP or 20 μM Dig-Ang, after which they were exposed to UVA light in a Rayonet chamber at 3 J/cm^2. Cells were then incubated in 10 μM CldU for 20 min and then in 100 μM IdU for 20 min. In experiments with inhibitors, cells were pretreated for 1 hr with compounds which were also included during CldU and IdU labeling.

In experiments to examine the possibility of parental strand replacement synthesis or monitor ICL unhooking, cells were incubated with 10 μM CldU for 48 hr to uniformly label DNA followed by 24 hr in 10 μM IdU. Cells were treated with TMP/UVA as above, followed by 40–60 min incubation with 10 μM EdU. After the replication labeling period cells were harvested by trypsinization and approximately 200 cells were mixed with lysis buffer (0.5% SDS in 200 mM Tris-HCl [pH 7.5], 50 mM EDTA) on a glass slide (NewComer Supply). After tilting, the slides were air-dried, fixed in 3:1 methanol/acetic acid, incubated in 2.5 M HCl for 60 min, neutralized in0.4 M Tris-HCl (pH 7.5) for 5 min, washed in PBS, and immunostained. Antibodies and dilutions were rat anti-BrdU (CldU), 1:200; Dylight 649 goat anti-rat, 1:100; mouse anti-BrdU (IdU), 1:40; and Dylight 488 goat anti-mouse, 1:100 and Qdot 655 goat anti-mouse 1: 2,500. EdU was detected by click chemistry with azidobiotin and displayed by a Qdot 565 streptavidin conjugate. Imaging was carried out using a Zeiss Axiovert 200M microscope with the Axio Vision software packages (Zeiss). The quantum dot signal was imaged with a Qdot 655 filter.

Protein recruitment to laser localized ICLs—Cells were seeded in a 35-mm glass bottom culture dish (MatTek) 2 days before an experiment to achieve 50%–60% confluence. They were incubated with 5 μM TMP, at 37°C for 20 min prior to laser treatment. The plates were placed in an environmental chamber mounted on a Nikon Eclipse TE2000 confocal microscope. The chamber was maintained at 37°C and flushed with humidified CO_2. Laser localized ICLs were introduced by exposing defined regions of interest (ROI, 4 × 20 pixels, 0.16 μm/pixel, visualized with a Plan Fluor × 60/1.25 numerical aperture oil objective) to a laser beam from an SRS NL100 nitrogen laser-pumped dye laser (Andor) that fired 3-ns pulses. The repetition rate was 10 Hz at 365 nm. The power was 0.7 nanowatts, measured at the back aperture of the x60 objective. The diffraction-limited spot size was ~300 nm. Cells were then fixed and stained with appropriate antibodies.

Effect of MCM2 S108A on Replication traverse frequency—Human cDNAs for MCM2 (WT and S108A mutant) were PCR amplified from plasmids pDC690 and pDC6914 (Cortez et al., 2004) using primers MCM2 FW-HinDIII and MCM2 Rev-XhoI, gel purified, digested with HindIII and XhoI and ligated to HinDIII/XhoI linearized pCMVFLAGNt vector to generate plasmids pFLA-MCM2 WT and pFLAG MCM2 S108A. These were sequenced and confirmed to express a FLAG tagged MCM2 protein upon transfection into HeLa cells by western blot (FLAG and MCM2 antibodies) and immunostaining (FLAG). To determine the effect of MCM2 S108A in traverse and PLA assays, on day 1 HeLa cells were transfected with MCM2 3′UTR siRNA (10 nM) using RNAimax according to the manufacturer's instructions, on day 2 cells were transfected with MCM2 3′UTR siRNA (10

nM) + pFLAG-MCM2 (WT or S108A) (1 μg) using Jet Prime transfection reagent, and on day 4 experiments were performed.

Integrity of ICLs on replication tracts—*XPD*−/− cells were incubated in the presence of 10 μM CldU for 2 replication cycles, and 10 μM IdU for one replication cycle to generate RED-GREEN parental strands. Cells were then treated with (5 μM) Dig-TMP/UVA and pulse labeled with a third analog, 100 μM EDU, for 1 hour. At this time a T0 sample was collected, followed by a pulse chase to take samples at 4 and 6.5 Hs after the EDU pulse. Samples were then lysed and the DNA sheared, stretched onto slides and immunostained to detect the thymidine analogs and the Dig (Huang et al., 2013).

QUANTIFICATION AND STATISTICAL ANALYSIS

PLA experiments were analyzed with Duolink Image analysis software (Sigma). Images were acquired at several focal planes through the thickness of the cell and imported onto Duolink Image analysis software. Cell and signal properties were optimized to quantify the number of PLA signals per cell nucleus and kept constant for the different fields and samples. Results were exported onto Sigma plot, where statistical significance was analyzed using the Mann-Whitney Rank sum test (NS: $p > 0.5$, significant: *** $p < 0.001$), and dot plots where generated. The number of fields and nuclei analyzed in each experiment can be found in Table S2.

For replication pattern frequency experiments images were analyzed on Axiovision software. On each field Cldu (IdU) tracts carrying a Dig dot were identified and classified into the different categories. The counts were reported and graphed in Excel. The bar graphs indicate the Mean ± SD. Statistical significance was analyzed using chi-square test on Sigmaplot (NS: $p > 0.5$, significant: *** $p < 0.001$). The number of fields and events analyzed in each experiment can be found in Table S1.

Supplementary Material

Refer to Web version on PubMed Central for supplementary material.

ACKNOWLEDGMENTS

This research was supported, in part, by the Intramural Research Program of the NIH, National Institute on Aging, United States (Z01-AG000746–08). J.H. is supported by the National Natural Science Foundations of China (21708007 and 31871365). L.L. is supported, in part, by CA190635 and CA193124-Project3. We thank David Cortez for the kind gift of plasmids pDC690 and pDC6914 and Magnar Bjørås for the *NEIL3* knockout cells.

REFERENCES

Abid Ali F, Renault L, Gannon J, Gahlon HL, Kotecha A, Zhou JC, Rueda D, and Costa A (2016). Cryo-EM structures of the eukaryotic replica-tive helicase bound to a translocation substrate. Nat. Commun 7, 10708. [PubMed: 26888060]

Amunugama R, Willcox S, Wu RA, Abdullah UB, El-Sagheer AH, Brown T, McHugh PJ, Griffith JD, and Walter JC (2018). Replication Fork Reversal during DNA Interstrand Crosslink Repair Requires CMG Unloading. Cell Rep. 23, 3419–3428. [PubMed: 29924986]

Andreassen PR, D'Andrea AD, and Taniguchi T (2004). ATR couples FANCD2 monoubiquitination to the DNA-damage response. Genes Dev. 18, 1958–1963. [PubMed: 15314022]

Bakker ST, Van de Vrugt HJ, Rooimans MA, Oostra AB, Steltenpool J, Delzenne-Goette E, Van der Wal A, Van der Valk M, Joenje H, te Riele H, and de Winter JP (2009). FANCM-deficient mice reveal unique features of Fanconi anemia complementation group M. Hum. Mol. Genet 18, 3484–3495. [PubMed: 19561169]

Ball HL, and Cortez D (2005). ATRIP oligomerization is required for ATR-dependent checkpoint signaling. J. Biol. Chem 280, 31390–31396. [PubMed: 16027118]

Bhagwat N, Olsen AL, Wang AT, Hanada K, Stuckert P, Kanaar R, D'Andrea A, Niedernhofer LJ, and McHugh PJ (2009). XPF-ERCC1 participates in the Fanconi anemia pathway of cross-link repair. Mol. Cell. Biol 29, 6427–6437. [PubMed: 19805513]

Blackford AN, Schwab RA, Nieminuszczy J, Deans AJ, West SC, and Niedzwiedz W (2012). The DNA translocase activity of FANCM protects stalled replication forks. Hum. Mol. Genet 21, 2005–2016. [PubMed: 22279085]

Bochman ML, and Schwacha A (2009). The Mcm complex: unwinding the mechanism of a replicative helicase. Microbiol. Mol. Biol. Rev 73, 652–683. [PubMed: 19946136]

Bogliolo M, Bluteau D, Lespinasse J, Pujol R, Vasquez N, d'Enghien CD, Stoppa-Lyonnet D, Leblanc T, Soulier J, and Surrallés J (2018). Biallelic truncating FANCM mutations cause early-onset cancer but not Fanconi anemia. Genet. Med 20, 458–463. [PubMed: 28837157]

Brosh RM Jr., Bellani M, Liu Y, and Seidman MM (2017). Fanconi Anemia: A DNA repair disorder characterized by accelerated decline of the hematopoietic stem cell compartment and other features of aging. Ageing Res. Rev 33, 67–75. [PubMed: 27223997]

Castella M, Jacquemont C, Thompson EL, Yeo JE, Cheung RS, Huang JW, Sobeck A, Hendrickson EA, and Taniguchi T (2015). FANCI Regulates Recruitment of the FA Core Complex at Sites of DNA Damage Independently of FANCD2. PLoS Genet. 11, e1005563. [PubMed: 26430909]

Catucci I, Osorio A, Arver B, Neidhardt G, Bogliolo M, Zanardi F, Riboni M, Minardi S, Pujol R, Azzollini J, et al. (2018). Individuals with FANCM biallelic mutations do not develop Fanconi anemia, but show risk for breast cancer, chemotherapy toxicity and may display chromosome fragility. Genet. Med 20, 452–457. [PubMed: 28837162]

Charych DH, Coyne M, Yabannavar A, Narberes J, Chow S, Wallroth M, Shafer C, and Walter AO (2008). Inhibition of Cdc7/Dbf4 kinase activity affects specific phosphorylation sites on MCM2 in cancer cells. J. Cell. Biochem 104, 1075–1086. [PubMed: 18286467]

Ciccia A, Ling C, Coulthard R, Yan Z, Xue Y, Meetei AR, Laghmani H, Joenje H, McDonald N, de Winter JP, et al. (2007). Identification of FAAP24, a Fanconi anemia core complex protein that interacts with FANCM. Mol. Cell 25, 331–343. [PubMed: 17289582]

Collis SJ, and Boulton SJ (2010). FANCM: fork pause, rewind and play. EMBO J. 29, 703–705. [PubMed: 20160754]

Collis SJ, Ciccia A, Deans AJ, Horejsí Z, Martin JS, Maslen SL, Skehel JM, Elledge SJ, West SC, and Boulton SJ (2008). FANCM and FAAP24 function in ATR-mediated checkpoint signaling independently of the Fanconi anemia core complex. Mol. Cell 32, 313–324. [PubMed: 18995830]

Cortez D, Glick G, and Elledge SJ (2004). Minichromosome maintenance proteins are direct targets of the ATM and ATR checkpoint kinases. Proc. Natl. Acad. Sci. USA 101, 10078–10083. [PubMed: 15210935]

Costa A, Ilves I, Tamberg N, Petojevic T, Nogales E, Botchan MR, and Berger JM (2011). The structural basis for MCM2–7 helicase activation by GINS and Cdc45. Nat. Struct. Mol. Biol 18, 471–477. [PubMed: 21378962]

Coster G, and Diffley JFX (2017). Bidirectional eukaryotic DNA replication is established by quasi-symmetrical helicase loading. Science 357, 314–318. [PubMed: 28729513]

Deans AJ, and West SC (2009). FANCM connects the genome instability disorders Bloom's Syndrome and Fanconi Anemia. Mol. Cell 36, 943–953. [PubMed: 20064461]

Fullbright G, Rycenga HB, Gruber JD, and Long DT (2016). p97 Promotes a Conserved Mechanism of Helicase Unloading during DNA Cross-Link Repair. Mol. Cell. Biol 36, 2983–2994. [PubMed: 27644328]

Garcia-Higuera I, Taniguchi T, Ganesan S, Meyn MS, Timers C, Hejna J, Grompe M, and D'Andrea AD (2001). Interaction of the Fanconi anemia proteins and BRCA1 in a common pathway. Mol. Cell 7, 249–262. [PubMed: 11239454]

Gari K, Décaillet C, Stasiak AZ, Stasiak A, and Constantinou A (2008). The Fanconi anemia protein FANCM can promote branch migration of Holliday junctions and replication forks. Mol. Cell 29, 141–148. [PubMed: 18206976]

Ge XQ, Jackson DA, and Blow JJ (2007). Dormant origins licensed by excess Mcm2–7 are required for human cells to survive replicative stress. Genes Dev. 21, 3331–3341. [PubMed: 18079179]

Geiduschek EP (1961). "Reversible" DNA. Proc. Natl. Acad. Sci. USA 47, 950–955. [PubMed: 13704192]

Georgescu R, Yuan Z, Bai L, de Luna Almeida Santos R, Sun J, Zhang D, Yurieva O, Li H, and O'Donnell ME (2017). Structure of eukaryotic CMG helicase at a replication fork and implications to replisome architecture and origin initiation. Proc. Natl. Acad. Sci. USA 114, E697–E706. [PubMed: 28096349]

Gérard A, Koundrioukoff S, Ramillon V, Sergère JC, Mailand N, Quivy JP, and Almouzni G (2006). The replication kinase Cdc7-Dbf4 promotes the interaction of the p150 subunit of chromatin assembly factor 1 with proliferating cell nuclear antigen. EMBO Rep. 7, 817–823. [PubMed: 16826239]

Hashimoto Y, Puddu F, and Costanzo V (2011). RAD51- and MRE11-dependent reassembly of uncoupled CMG helicase complex at collapsed replication forks. Nat. Struct. Mol. Biol 19, 17–24. [PubMed: 22139015]

Horejší Z, Collis SJ, and Boulton SJ (2009). FANCM-FAAP24 and HCLK2: roles in ATR signalling and the Fanconi anemia pathway. Cell Cycle 8, 1133–1137. [PubMed: 19282663]

Huang M, Kim JM, Shiotani B, Yang K, Zou L, and D'Andrea AD (2010). The FANCM/FAAP24 complex is required for the DNA interstrand crosslink-induced checkpoint response. Mol. Cell 39, 259–268. [PubMed: 20670894]

Huang J, Liu S, Bellani MA, Thazhathveetil AK, Ling C, de Winter JP, Wang Y, Wang W, and Seidman MM (2013). The DNA translocase FANCM/MHF promotes replication traverse of DNA interstrand crosslinks. Mol. Cell 52, 434–446. [PubMed: 24207054]

Kelsall IR, Langenick J, MacKay C, Patel KJ, and Alpi AF (2012). The Fanconi anaemia components UBE2T and FANCM are functionally linked to nucleotide excision repair. PLoS One 7, e36970. [PubMed: 22615860]

Kim JM, Kee Y, Gurtan A, and D'Andrea AD (2008). Cell cycle-dependent chromatin loading of the Fanconi anemia core complex by FANCM/FAAP24. Blood 111, 5215–5222. [PubMed: 18174376]

Klein Douwel D, Boonen RA, Long DT, Szypowska AA, Räschle M, Walter JC, and Knipscheer P (2014). XPF-ERCC1 acts in Unhooking DNA interstrand crosslinks in cooperation with FANCD2 and FANCP/SLX4. Mol. Cell 54, 460–471. [PubMed: 24726325]

Knipscheer P, Räschle M, Schärer OD, and Walter JC (2012). Replication-coupled DNA interstrand cross-link repair in Xenopus egg extracts. Methods Mol. Biol 920, 221–243. [PubMed: 22941607]

Li H, and O'Donnell ME (2018). The Eukaryotic CMG Helicase at the Replication Fork: Emerging Architecture Reveals an Unexpected Mechanism. BioEssays 40.

Li N, Zhai Y, Zhang Y, Li W, Yang M, Lei J, Tye BK, and Gao N (2015). Structure of the eukaryotic MCM complex at 3.8Å. Nature 524, 186–191. [PubMed: 26222030]

Ling C, Huang J, Yan Z, Li Y, Ohzeki M, Ishiai M, Xu D, Takata M, Seidman M, and Wang W (2016). Bloom syndrome complex promotes FANCM recruitment to stalled replication forks and facilitates both repair and traverse of DNA interstrand crosslinks. Cell Discov. 2, 16047. [PubMed: 28058110]

Long DT, Joukov V, Budzowska M, and Walter JC (2014). BRCA1 promotes unloading of the CMG helicase from a stalled DNA replication fork. Mol. Cell 56, 174–185. [PubMed: 25219499]

Lossaint G, Larroque M, Ribeyre C, Bec N, Larroque C, Décaillet C, Gari K, and Constantinou A (2013). FANCD2 binds MCM proteins and controls replisome function upon activation of s phase checkpoint signaling. Mol. Cell 51, 678–690. [PubMed: 23993743]

Mamrak NE, Shimamura A, and Howlett NG (2017). Recent discoveries in the molecular pathogenesis of the inherited bone marrow failure syndrome Fanconi anemia. Blood Rev. 31, 93–99. [PubMed: 27760710]

Marmur J, and Grossman L (1961). Ultraviolet light induced linking of deoxyribonucleic acid strands and its reversal by photoreactivating enzyme. Proc. Natl. Acad. Sci. USA 47, 778–787. [PubMed: 13767019]

Matsuoka S, Ballif BA, Smogorzewska A, McDonald ER 3rd, Hurov KE, Luo J, Bakalarski CE, Zhao Z, Solimini N, Lerenthal Y, et al. (2007). ATM and ATR substrate analysis reveals extensive protein networks responsive to DNA damage. Science 316, 1160–1166. [PubMed: 17525332]

Meetei AR, Medhurst AL, Ling C, Xue Y, Singh TR, Bier P, Stelten-pool J, Stone S, Dokal I, Mathew CG, et al. (2005). A human ortholog of archaeal DNA repair protein Hef is defective in Fanconi anemia complementation group M. Nat. Genet 37, 958–963. [PubMed: 16116422]

Mijic S, Zellweger R, Chappidi N, Berti M, Jacobs K, Mutreja K, Ursich S, Ray Chaudhuri A, Nussenzweig A, Janscak P, and Lopes M (2017). Replication fork reversal triggers fork degradation in BRCA2-defective cells. Nat. Commun 8, 859. [PubMed: 29038466]

Muniandy PA, Thapa D, Thazhathveetil AK, Liu ST, and Seidman MM (2009). Repair of laser-localized DNA interstrand cross-links in G1 phase mammalian cells. J. Biol. Chem 284, 27908–27917. [PubMed: 19684342]

Mutreja K, Krietsch J, Hess J, Ursich S, Berti M, Roessler FK, Zellweger R, Patra M, Gasser G, and Lopes M (2018). ATR-Mediated Global Fork Slowing and Reversal Assist Fork Traverse and Prevent Chromosomal Breakage at DNA Interstrand Cross-Links. Cell Rep. 24, 2629–2642.e5. [PubMed: 30184498]

Niedernhofer LJ, Daniels JS, Rouzer CA, Greene RE, and Marnett LJ (2003). Malondialdehyde, a product of lipid peroxidation, is mutagenic in human cells. J. Biol. Chem 278, 31426–31433. [PubMed: 12775726]

O'Donnell ME, and Li H (2018). The ring-shaped hexameric helicases that function at DNA replication forks. Nat. Struct. Mol. Biol 25, 122–130. [PubMed: 29379175]

Pan X, Drosopoulos WC, Sethi L, Madireddy A, Schildkraut CL, and Zhang D (2017). FANCM, BRCA1, and BLM cooperatively resolve the replication stress at the ALT telomeres. Proc. Natl. Acad. Sci. USA 114, E5940–E5949. [PubMed: 28673972]

Pontel LB, Rosado IV, Burgos-Barragan G, Garaycoechea JI, Yu R, Arends MJ, Chandrasekaran G, Broecker V, Wei W, Liu L, et al. (2015). Endogenous Formaldehyde Is a Hematopoietic Stem Cell Genotoxin and Metabolic Carcinogen. Mol. Cell 60, 177–188. [PubMed: 26412304]

Price NE, Li L, Gates KS, and Wang Y (2017). Replication and repair of a reduced 2′-deoxyguanosine-abasic site interstrand cross-link in human cells. Nucleic Acids Res. 45, 6486–6493. [PubMed: 28431012]

Räschle M, Knipscheer P, Enoiu M, Angelov T, Sun J, Griffith JD, Ellenberger TE, Schärer OD, and Walter JC (2008). Mechanism of replication-coupled DNA interstrand crosslink repair. Cell 134, 969–980. [PubMed: 18805090]

Rohleder F, Huang J, Xue Y, Kuper J, Round A, Seidman M, Wang W, and Kisker C (2016). FANCM interacts with PCNA to promote replication traverse of DNA interstrand crosslinks. Nucleic Acids Res. 44, 3219–3232. [PubMed: 26825464]

Rolseth V, Luna L, Olsen AK, Suganthan R, Scheffler K, Neurauter CG, Esbensen Y, Ku snierczyk A, Hildrestrand GA, Graupner A, Andersen JM, Slupphaug G, Klungland A, Nilsen H, and Bjørås M (2017). No cancer predisposition or increased spontaneous mutation frequencies in NEIL DNA glycosylases-deficient mice. Sci. Rep 7, 4384. [PubMed: 28663564]

Rupp WD, and Howard-Flanders P (1968). Discontinuities in the DNA synthesized in an excision-defective strain of Escherichia coli following ultraviolet irradiation. J. Mol. Biol 31, 291–304. [PubMed: 4865486]

Saldivar JC, Cortez D, and Cimprich KA (2017). The essential kinase ATR: ensuring faithful duplication of a challenging genome. Nat. Rev. Mol. Cell Biol 18, 622–636. [PubMed: 28811666]

Sareen A, Chaudhury I, Adams N, and Sobeck A (2012). Fanconi anemia proteins FANCD2 and FANCI exhibit different DNA damage responses during S-phase. Nucleic Acids Res. 40, 8425–8439. [PubMed: 22753026]

Schlacher K, Wu H, and Jasin M (2012). A distinct replication fork protection pathway connects Fanconi anemia tumor suppressors to RAD51-BRCA1/2. Cancer Cell 22, 106–116. [PubMed: 22789542]

Semlow DR, Zhang J, Budzowska M, Drohat AC, and Walter JC (2016). Replication-Dependent Unhooking of DNA Interstrand Cross-Links by the NEIL3 Glycosylase. Cell 167, 498–511.e14. [PubMed: 27693351]

Singh TR, Ali AM, Paramasivam M, Pradhan A, Wahengbam K, Seidman MM, and Meetei AR (2013). ATR-dependent phosphorylation of FANCM at serine 1045 is essential for FANCM functions. Cancer Res. 73, 4300–4310. [PubMed: 23698467]

Sobeck A, Stone S, Landais I, de Graaf B, and Hoatlin ME (2009). The Fanconi anemia protein FANCM is controlled by FANCD2 and the ATR/ATM pathways. J. Biol. Chem 284, 25560–25568. [PubMed: 19633289]

Söderberg O, Leuchowius KJ, Gullberg M, Jarvius M, Weibrecht I, Lars-son LG, and Landegren U (2008). Characterizing proteins and their interactions in cells and tissues using the in situ proximity ligation assay. Methods 45, 227–232. [PubMed: 18620061]

Sumpter R Jr., and Levine B (2017). Emerging functions of the Fanconi anemia pathway at a glance. J. Cell Sci 130, 2657–2662. [PubMed: 28811338]

Tacconi EM, Lai X, Folio C, Porru M, Zonderland G, Badie S, Michl J, Sechi I, Rogier M, Matía García V, et al. (2017). BRCA1 and BRCA2 tumor suppressors protect against endogenous acetaldehyde toxicity. EMBO Mol. Med 9, 1398–1414. [PubMed: 28729482]

Taylor MRG, and Yeeles JTP (2018). The Initial Response of a Eukaryotic Replisome to DNA Damage. Mol. Cell 70, 1067–1080.e12. [PubMed: 29944888]

Thazhathveetil AK, Liu ST, Indig FE, and Seidman MM (2007). Psoralen conjugates for visualization of genomic interstrand cross-links localized by laser photoactivation. Bioconjug. Chem 18, 431–437. [PubMed: 17373769]

Thompson EL, Yeo JE, Lee EA, Kan Y, Raghunandan M, Wiek C, Hanenberg H, Schärer OD, Hendrickson EA, and Sobeck A (2017). FANCI and FANCD2 have common as well as independent functions during the cellular replication stress response. Nucleic Acids Res. 45, 11837–11857. [PubMed: 29059323]

Tian Y, Shen X, Wang R, Klages-Mundt NL, Lynn EJ, Martin SK, Ye Y, Gao M, Chen J, Schlacher K, and Li L (2017). Constitutive role of the Fanconi anemia D2 gene in the replication stress response. J. Biol. Chem 292, 20184–20195. [PubMed: 29021208]

Wang Y, Leung JW, Jiang Y, Lowery MG, Do H, Vasquez KM, Chen J, Wang W, and Li L (2013). FANCM and FAAP24 maintain genome stability via cooperative as well as unique functions. Mol. Cell 49, 997–1009. [PubMed: 23333308]

Weber CA, Salazar EP, Stewart SA, and Thompson LH (1988). Molecular cloning and biological characterization of a human gene, ERCC2, that corrects the nucleotide excision repair defect in CHO UV5 cells. Mol. Cell Biol 8, 1137–1146. [PubMed: 2835663]

Wiegant WW, Overmeer RM, Godthelp BC, van Buul PP, and Zdzienicka MZ (2006). Chinese hamster cell mutant, V-C8, a model for analysis of Brca2 function. Mutat. Res 600, 79–88. [PubMed: 16643964]

Williams HL, Gottesman ME, and Gautier J (2012). Replication-independent repair of DNA interstrand crosslinks. Mol. Cell 47, 140–147. [PubMed: 22658724]

Xue Y, Li Y, Guo R, Ling C, and Wang W (2008). FANCM of the Fanconi anemia core complex is required for both monoubiquitination and DNA repair. Hum. Mol. Genet 17, 1641–1652. [PubMed: 18285517]

Yamamoto K, Hirano S, Ishiai M, Morishima K, Kitao H, Namikoshi K, Kimura M, Matsushita N, Arakawa H, Buerstedde JM, et al. (2005). Fanconi anemia protein FANCD2 promotes immunoglobulin gene conversation and DNA repair through a mechanism related to homologous recombination. Mol. Cell Biol 25, 34–43. [PubMed: 15601828]

Yamamoto KN, Kobayashi S, Tsuda M, Kurumizaka H, Takata M, Kono K, Jiricny J, Takeda S, and Hirota K (2011). Involvement of SLX4 in inter-strand cross-link repair is regulated by the Fanconi anemia pathway. Proc. Natl. Acad. Sci. USA 108, 6492–6496. [PubMed: 21464321]

Yan Z, Delannoy M, Ling C, Daee D, Osman F, Muniandy PA, Shen X, Oostra AB, Du H, Steltenpool J, et al. (2010). A histone-fold complex and FANCM form a conserved DNA-remodeling complex to maintain genome stability. Mol. Cell 37, 865–878. [PubMed: 20347428]

Yang Z, Nejad MI, Varela JG, Price NE, Wang Y, and Gates KS (2017). A role for the base excision repair enzyme NEIL3 in replication-dependent repair of interstrand DNA cross-links derived from psoralen and abasic sites. DNA Repair (Amst.) 52, 1–11. [PubMed: 28262582]

Yeeles JT, and Marians KJ (2011). The Escherichia coli replisome is inherently DNA damage tolerant. Science 334, 235–238. [PubMed: 21998391]

Yeeles JT, Deegan TD, Janska A, Early A, and Diffley JF (2015). Regulated eukaryotic DNA replication origin firing with purified proteins. Nature 519, 431–435. [PubMed: 25739503]

Zellweger R, Dalcher D, Mutreja K, Berti M, Schmid JA, Herrador R, Vindigni A, and Lopes M (2015). Rad51-mediated replication fork reversal is a global response to genotoxic treatments in human cells. J. Cell Biol 208, 563–579. [PubMed: 25733714]

Zhai Y, and Tye BK (2017). Structure of the MCM2–7 Double Hexamer and Its Implications for the Mechanistic Functions of the Mcm2–7 Complex. Adv. Exp. Med. Biol 1042, 189–205. [PubMed: 29357059]

Zhang J, Dewar JM, Budzowska M, Motnenko A, Cohn MA, and Walter JC (2015). DNA interstrand cross-link repair requires replication-fork convergence. Nat. Struct. Mol. Biol 22, 242–247. [PubMed: 25643322]

Highlights

- The eukaryotic replication helicase (CMG) composition changes when blocked by an ICL
- FANCM associates with the CDC45-MCM complex while the GINS are released
- ATR, FANCD2, and the translocase activity of FANCM contribute to replication past the ICL

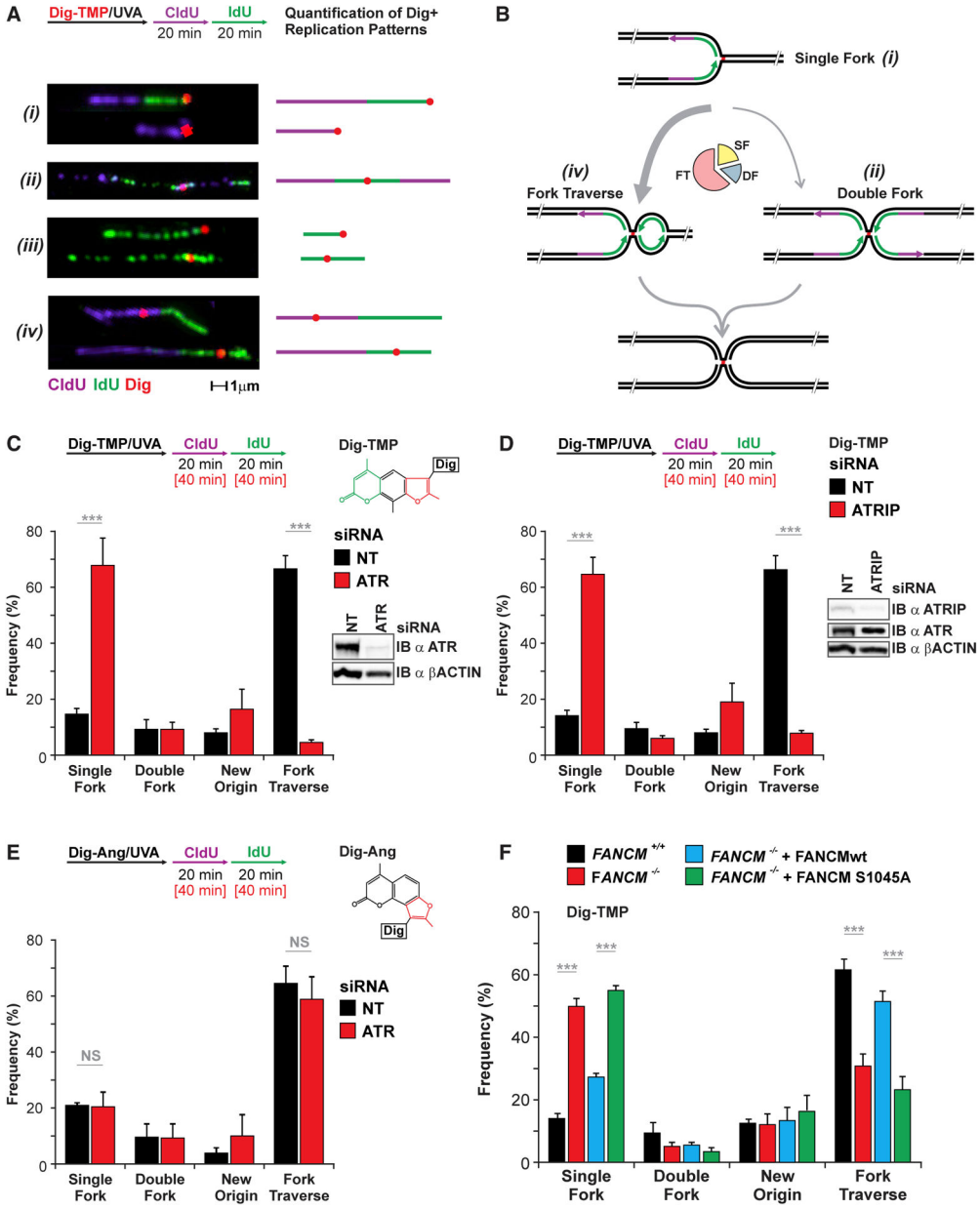

Figure 1. Phosphorylation of FANCM by ATR Is Required for Replication Traverse

(A) Fiber patterns showing replication tracts in the vicinity of Dig-TMP ICLs.

(B) Interpretation of the patterns. The pie chart shows the relative frequency of the major patterns in wild-type (WT) cells. RT, replication traverse; SF, single fork; DF, double fork.

(C–F) Replication patterns in cells (C) in which ATR expression was suppressed by siRNA; (D) treated with siRNA against ATRIP; (E) treated with siRNA against ATR and exposed to Dig-Ang; and (F) in WT or FANCM-deficient cells, or FANCM-deficient cells complemented with WT FANCM or a phosphorylation resistant variant (S1045). Data are presented as mean ± SD (***$p < 0.001$, chi-square test).

See also Figure S1 and Table S1.

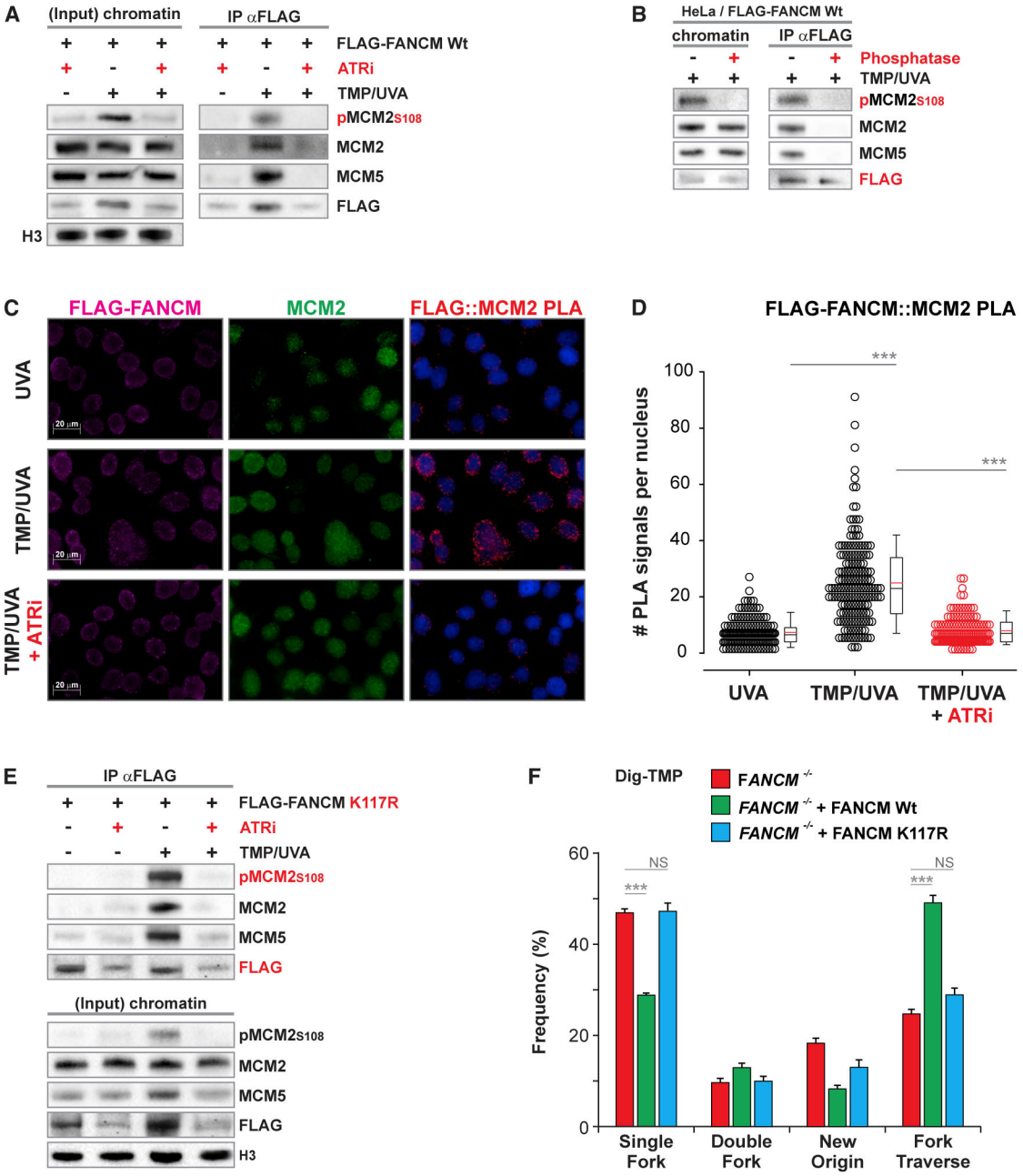

Figure 2. FANCM Interacts with the MCM Complex

(A) Cells expressing FLAG FANCM were treated with UVA or TMP/UVA and incubated for 1 h with or without ATR inhibitor (ATRi) VE-821. Chromatin proteins were prepared and either analyzed directly (chromatin) or incubated with anti-FLAG antibody linked to magnetic beads. Bound proteins were analyzed by western blotting.

(B) Binding of MCM proteins by FANCM requires phosphorylation. Samples were treated with calf intestine alkaline phosphatase.

(C) PLA between FLAG-FANCM and MCM2. Cells expressing FLAG-FANCM were either exposed to UVA only or treated with TMP/UVA or TMP/UVA and VE-821. After 1 h the cells were fixed, and the PLA between FANCM and MCM2 determined.

(D) Quantification of (C). ***p < 0.001 (rank-sum test).

(E) ATR-dependent binding of the MCM complex by the FANCM translocase mutant K117R in cells exposed to TMP/UVA.

(F) Traverse frequency is reduced in *FANCM* knockout cells expressing FANCM K117R. Data are presented as mean ± SD (not significant [NS], p > 0.05; ***p < 0.001; chi-square test). See also Figure S2 and Tables S1 and S2.

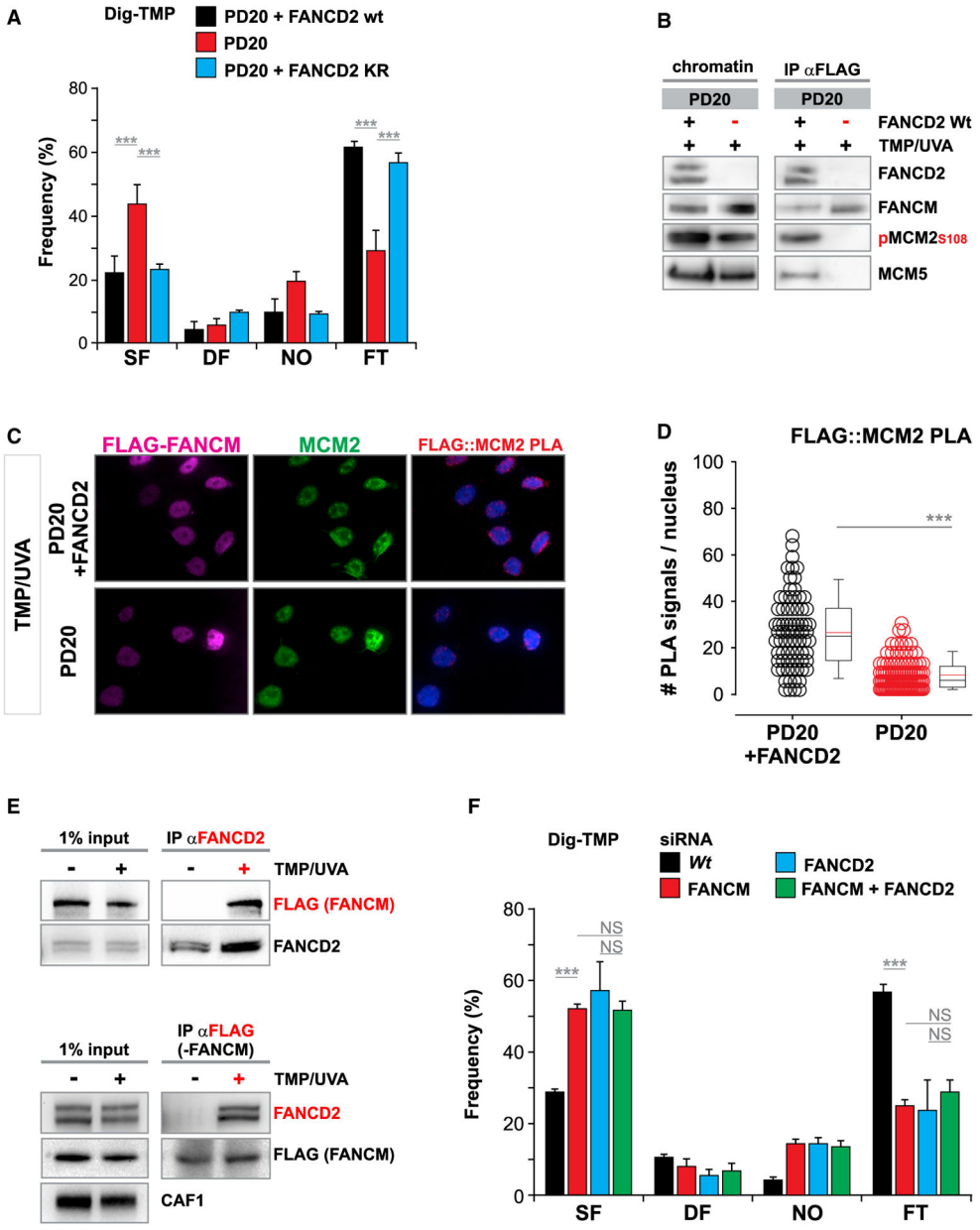

Figure 3. FANCD2 Is Epistatic with FANCM in Support of Replication Traverse

(A) Replication patterns in FANCD2-deficient PD20 cells or PD20 cells complemented with WT FANCD2 or the ubiquitin-resistant K561R variant.

(B) Association of FANCM with MCM proteins is dependent on FANCD2. PD20 cells or PD20 cells complemented by expression of WT FANCD2 were transfected with a plasmid expressing WT FLAG-FANCM, followed by treatment as indicated and coIP from a preparation of chromatin proteins.

(C) PLA between FLAG-FANCM and MCM2 in PD20 cells, or PD20 cells expressing WT FANCD2.

(D) Quantification of (C). ***$p < 0.001$ (rank-sum test).

(E) coIP between FANCM and FANCD2 from chromatin proteins from cells treated with TMP/UVA.

(F) *FANCM* and *FANCD2* are epistatic in replication traverse. (A and F) Data are presented as mean ± SD (NS, $p > 0.05$; ***$p < 0.001$; chi-square test).

See also Figure S3 and Tables S1 and S2.

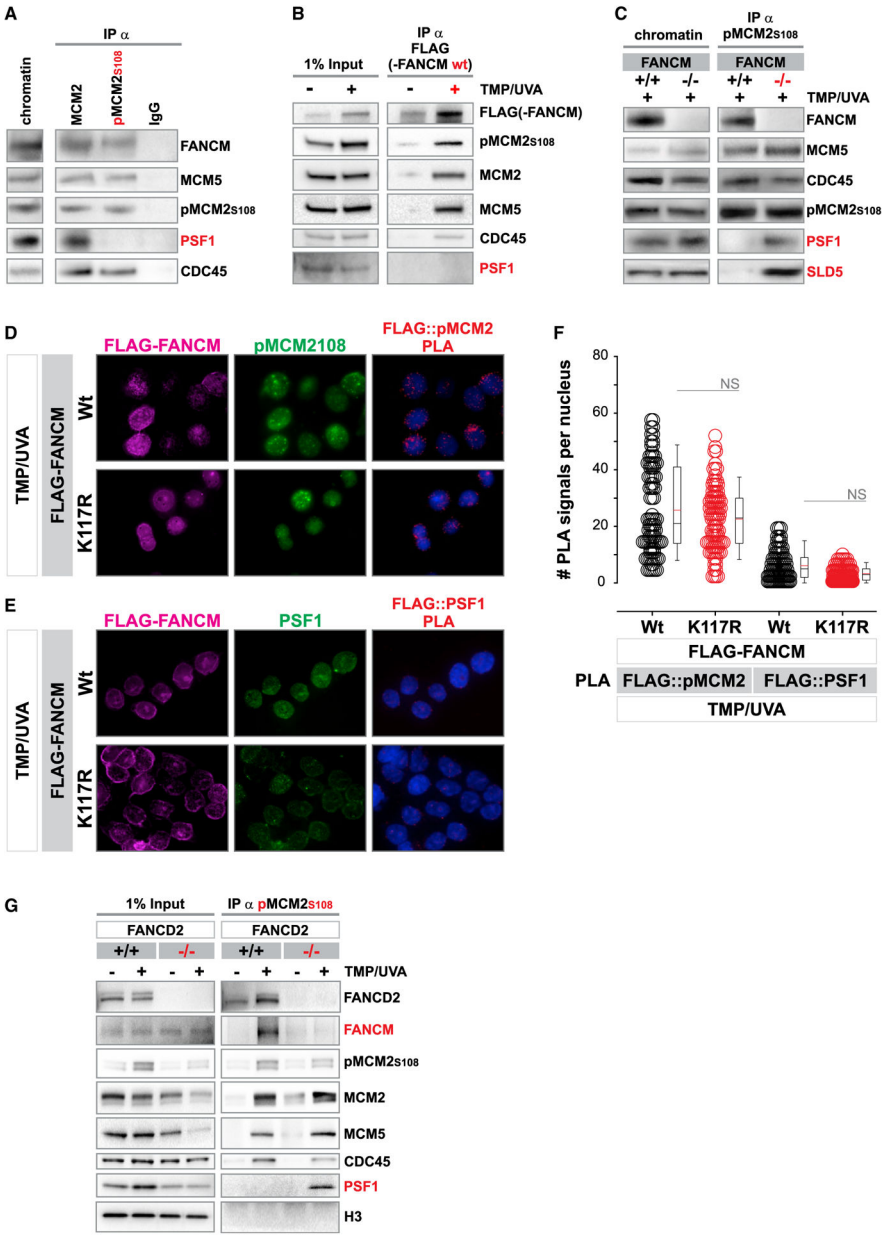

Figure 4. FANCM Association with MCM Proteins Is Coincident with Release of GINS Proteins

(A) coIP against MCM2 or phospho-MCM2S108 after treatment of cells with TMP/UVA.

(B) coIP against FLAG-FANCM in cells with or without treatment with TMP/UVA.

(C) Inverse correlation between GINS and FANCM association with CMG complex. coIP against pMCM2S108 chromatin proteins from FANCM-expressing or -deficient cells, treated with TMP/UVA.

(D) PLA between WT or translocase inactive (K117R) FANCM pMCM2S108.

(E) PLA between WT or translocase inactive (K117R) FANCM and PSF1 (GINS1).

(F) Quantification of (D) and (E). Data are presented as mean ± SD. NS, $p > 0.05$ (rank-sum test).

(G) FANCD2 is required for the interaction between FANCM and the MCM complex defined by phospho-MCM2. coIP between pMCM2 and chromatin proteins in *FANCD2* knockout cells or knockout cells expressing WT FANCD2.
See also Figure S4 and Table S2.

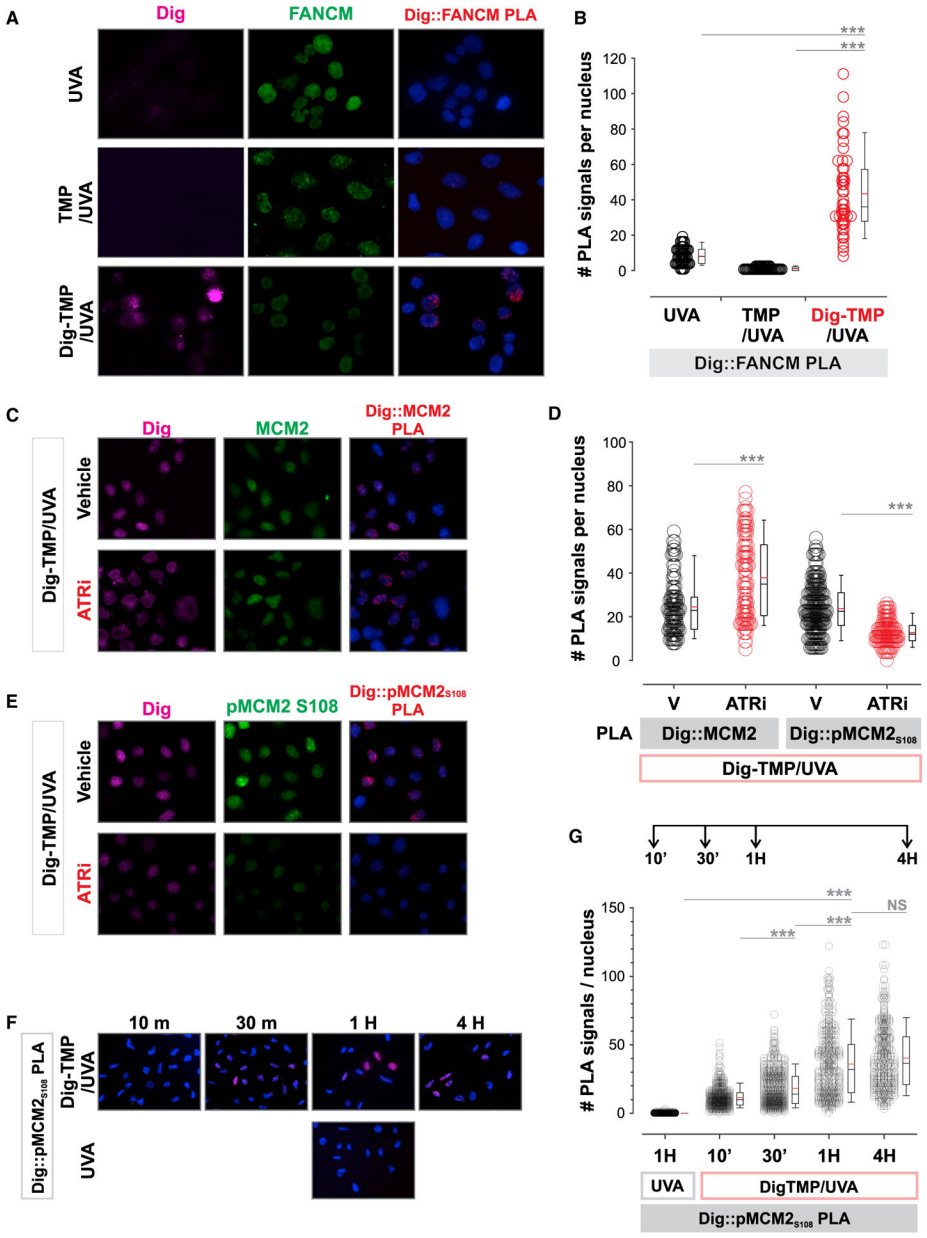

Figure 5. The Interaction of CMG Proteins with ICLs Is Regulated by ATR

(A) PLA between Dig tag on the ICLs and FANCM. Cells were treated with UVA, TMP/UVA, or Dig-TMP/UVA and, after 1-h incubation at 37°C, fixed and PLA between Dig and FANCM performed. The UVA and TMP/UVA provide controls for non-specific binding in cells exposed to UVA or TMP/UVA stress.

(B) Quantification of (A).

(C) PLA between Dig-TMP and MCM2. In addition to Dig-TMP/UVA, cells were treated with either DMSO or VE-821 in DMSO.

(D) Quantification of (C) and (E).

(E) PLA between Dig-TMP and pMCM2S108.

(F) Time course of PLA between Dig-TMP and pMCM2S108.

Data are presented as mean ± SD. Control cells were exposed to UVA in the absence of Dig-TMP and incubated for 1 h prior to the PLA.

(G) Quantification of (F).

(B, D, and G) Data are presented as mean ± SD. NS, $p > 0.05$; ***$p < 0.001$ (rank-sum test). See also Figure S5 and Table S2.

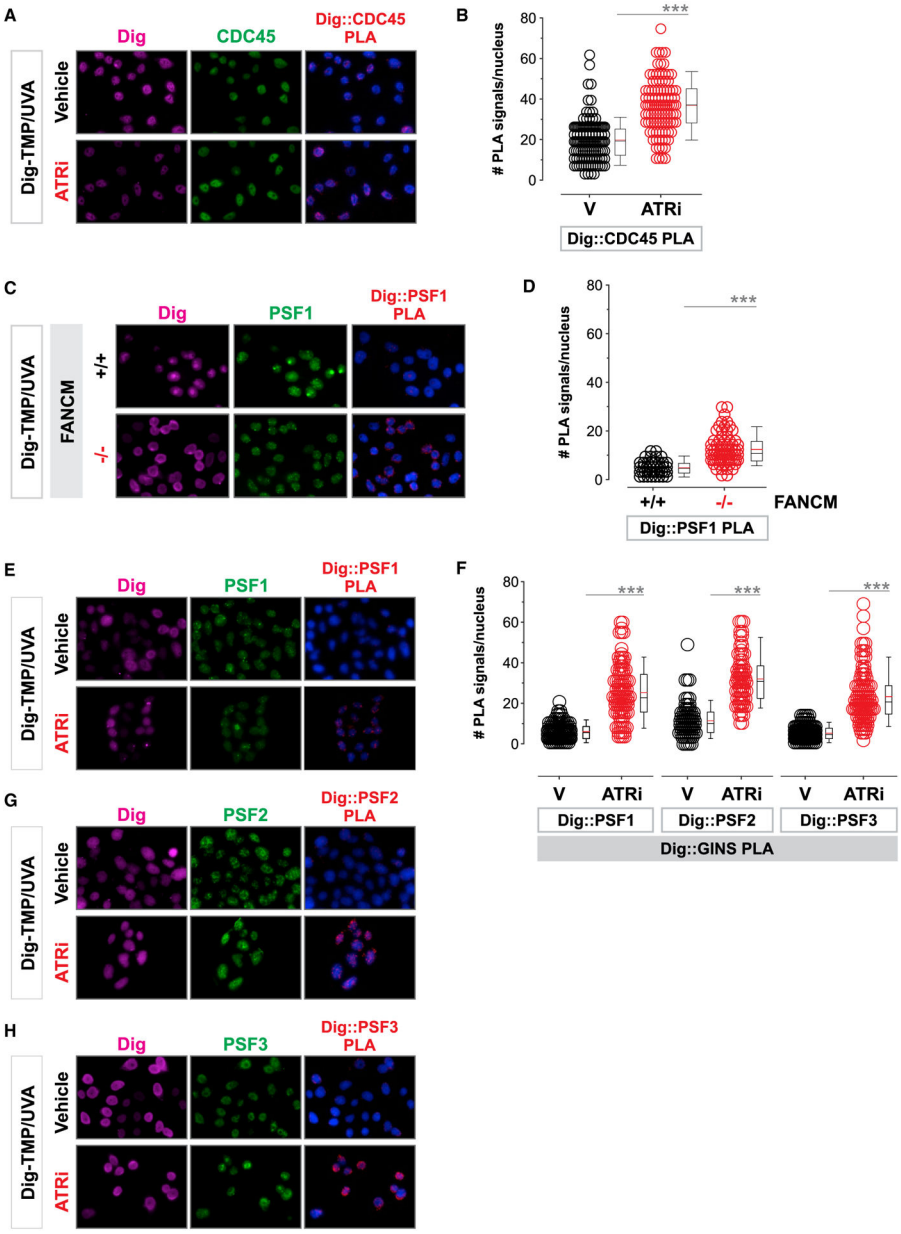

Figure 6. The Loss of GINS from Replisomes at ICLs Is Dependent on ATR and FANCM

Cells were treated with Dig-TMP/UVA, incubated for an hour, and then PLA performed between the indicated protein and Dig.

(A) PLA between Dig and CDC45 in the presence or absence of VE-821 or DMSO (V).

(B) Quantification of (A).

(C) PLA between Dig and PSF1 in FANCM $^{+}$ or $^{-}$ cells.

(D) Quantification of (E), (G), and (H).

(E) PLA between Dig and PSF1, +/− VE-821.

(F) Quantification of (E), (G), and (H).

(G) PLA between Dig and PSF2, +/− VE-821.

(H) PLA between Dig and PSF3, +/− VE-821.

(B, D, and F) Data are presented as mean ± SD. ***p < 0.001 (rank-sum test). See also Figure S6 and Table S2.

KEY RESOURCES TABLE

REAGENT or RESOURCE	SOURCE	IDENTIFIER
Antibodies		
Rabbit anti 53BP1	Novus	Cat# NB100–304; RRID:AB_10003037
Rabbit polyclonal anti ATR	Abeam	Cat# ab2905; RRID:AB_303400
Rabbit anti ATRIP	Abeam	Cat#ab175221; RRID: N/A
Rabbit mAb anti β-actin	Cell Signaling Technology	Cat# 4970; RRID:AB_2223172
Mouse mAb anti β-actin	Sigma	Cat#A5316; RRID:AB_476743
Rat mAb anti-BrdU (detecting CldU)	Abeam	Cat# ab6326; RRID:AB_305426
mouse anti-BrdU (detecting IdU)	BD Biosciences	Cat# 347580; RRID:AB_400326
Rabbit anti p150 (CAF1)	Abeam	Cat# ab126625; RRID:AB_11131934
RabMAb anti CDC45	Abeam	Cat# ab126762; RRID:AB_11140216
Mouse monoclonal anti Digoxigenin	Abeam	Cat# ab420; RRID:AB_304362
Rabbit oligoclonal anti Digoxigenin	Invitrogen	Cat# 710019; RRID:AB_2532530
Rabbit anti FAAP24	Weidong Wang Lab	Ciccia et al., 2007
Rabbit polyclonal anti FANCD2	Novus	Cat# NB100–182; RRID:AB_10002867
Rabbit polyclonal anti FANCM	Weidong Wang Lab	Meetei et al., 2005
Rabbit monoclonal anti FLAG	Sigma	Cat# F2555; RRID:AB_796202
Anti-FLAG® M2 Magnetic Beads	Sigma	Cat# M8823; RRID:AB_2637089
Rabbit anti H3	Abeam	Cat# ab1791; RRID:AB_302613
Rabbit anti MCM2	Abeam	Cat# ab4461; RRID:AB_304470
Rabbit anti MCM5	Abeam	Cat# ab17967; RRID:AB_444144
Rabbit anti MHF1	Weidong Wang Lab	Yan et al., 2010
AF488-mouse anti PCNA	Abeam	Cat#ab201672; RRID N/A
Mouse mAb anti PCNA	Abeam	Cat# ab29; RRID:AB_303394
Rabbit anti phosphoMCM2S108	Abeam	Cat# ab109271; RRID:AB_10891758
Rabbit anti PSF1	Abeam	Cat#ab181112; RRID N/A
Rabbit anti RAD51	Abeam	Cat# ab63801; RRID:AB_1142428
Rabbit anti SLD5	Bethyl Labs	Cat#A304–141A; RRID:AB_2621390

REAGENT or RESOURCE	SOURCE	IDENTIFIER
Mouse anti SLX4	Novus	Cat# H00084464-B01P; RRID:AB_2067349
AF488-Goat anti mouse IgG	ThermoFisher	Cat#A-11001; RRID:AB_2534069
Qdot655-Goat anti rabbit IgG	ThermoFisher	Cat#Q-11421MP; RRID:AB_1500767
AF633-Goat anti Rat IgG	ThermoFisher	Cat#A-21094; RRID:AB_2535749
AF568-StreptAvidin conjugate	ThermoFisher	Cat# S-11226; RRID:AB_2315774
Biotin-goat anti StreptAvidin	Vector Labs	Cat# BA-0500; RRID:AB_2336221
Chemicals, Peptides, and Recombinant Proteins		
CldU	Sigma	C6891; RRID N/A
IdU	Sigma	17125; RRID N/A
EdU	Sigma	900584; RRID N/A
Azidobiotin	Click Chemistry Tools LLC.	AZ104–25; RRID N/A
Digoxigenin succinyl ester	Roche	11333054001; RRID N/A
Trimethyl psoralen (TMP)	Sigma	T6137; RRID NA
Digoxigenin trimethyl psoralen	This work	Thazhathveetil et al., 2007
Digoxigenin angelicin	This work	Thazhathveetil et al., 2007
Diamino glycol (4,7,10-Trioxa-1,13-tridecanediamine)	Sigma	369519; RRID N/A
Chlorination reagent (4’-Chloromethyl-4,5’, 8-trimethylprosalen)	Berry and Associates	PS5000; RRID N/A
VE821	Selleckchem	S8007; RRID N/A
XL413	Selleckchem	S7547; RRID N/A
PolyJetTM DNA Transfection Reagent	SignaGen Laboratories	SL100688; RRID N/A
a-Amanitin	Tocris	4025; RRID N/A
Critical Commercial Assays		
Duolink insitu Detection Reagent FarRed	Sigma	DUO92013–100RXN; RRID N/A
Duolink insitu PLA probe Anti mouse MINUS	Sigma	DUO92004–100RXN; RRID N/A
Duolink insitu PLA probe Anti Rabbit PLUS	Sigma	DUO92002–100RXN; RRID N/A
Duolink insitu wash buffers	Sigma	DUO82049–4L; RRID N/A
Experimental Models: Cell Lines		
Chicken: *FANCD2* $^{-/-}$ DT40 female chicken lymphoma derived	Weidong Wang Lab	Yamamoto et al., 2005
Chicken: *FANCD2* $^{+/+}$ DT40 female chicken lymphoma derived	Weidong Wang Lab	Yamamoto et al., 2005

Cell Rep. Author manuscript; available in PMC 2019 August 02.

REAGENT or RESOURCE	SOURCE	IDENTIFIER
Chicken: *FAAP24* $^{-/-}$ DT40 female chicken lymphoma derived	This paper	N/A
Hamster: *BRCA2* $^{-/-}$ CHO, female	Thompson Lab	Wiegant et al., 2006
Hamster: *XPD* $^{-/-}$ CHO, female	Thompson Lab	Weber et al., 1988
Human: 293, female	ATCC	ATCC CRL-1573, RRID:CVCL_0045
Human: PD20F: male fibroblasts *FANCD2* hypomorph	D'Andrea Lab	Garcia-Higuera et al., 2001
Human: PD20 complemented with FANCD2 Wt, male	D'Andrea Lab	Garcia-Higuera et al., 2001
Human: PD20 complemented with FANCD2 K561R mutant, male	D'Andrea Lab	Garcia-Higuera et al., 2001
Human: HeLa *FANCM* $^{-/-}$, female	This paper	N/A
Human: HeLa *FANCM* $^{+/+}$, female	This paper	N/A
Human: HeLa *FANCI* $^{-/-}$, female	Lei Li lab	Tian et al., 2017
Human: HeLa *FANCD2* $^{-/-}$, female	Lei Li lab	Tian et al., 2017
Human: HeLa *FANCD2* $^{-/-}$ *FANCI* $^{-/-}$, female	Lei Li lab	Tian et al., 2017
Human: HeLa *FANCD2* $^{+/+}$ *FANCI* $^{+/+}$, female	Lei Li lab	Tian et al., 2017
Human: *BRCA1* $^{-/-}$, female	ATCC	ATCC Cat# CRL-2336; RRID:CVCL_0290
Mouse: *NEIL3* $^{-/-}$ mouse embryonic fibroblasts (sex unknown, embryos not assessed for sex)	Magnar Bjoras lab	Rolseth et al., 2017
Mouse: *NEILS* $^{+/+}$ mouse embryonic fibroblasts (sex unknown, embryos not assessed for sex)	Magnar Bjoras lab	Rolseth et al., 2017
Mouse: *FANCM* $^{-/-}$ mouse embryonic fibroblasts, male	Weidong Wang Lab	Bakker et al., 2009
Mouse: *FANCM* $^{+/+}$ mouse embryonic fibroblasts, male	Weidong Wang Lab	Bakker et al., 2009
Mouse: *FANCM* $^{-/-}$ expressing FANCM S1045A, male	Weidong Wang Lab	Singh et al., 2013
Oligonucleotides		
ATR siRNA (AACCUCCGUGAUGUUGCUUGA)	Dharmaeon	Ball et al., 2005
ATRIP siRNA (AAGGUCCACAGAUUAUUAGAU)	Dharmaeon	Ball et al., 2005
FANCM siRNA (CUAUGCUUAUUGCCAGGUU)	Dharmaeon	Meetei et al., 2005
FANCD2 ON-Target plus siRNA SMART pool	Dharmaeon	L-016376–00-0005
SLX4 siRNA (AAACgUgAAUgAAgCAgAAUU)	Dharmaeon	N/A
3′UTR MCM2 siRNA (AAGGAUUCCUUGGGAUUCUGG)	Dharmaeon	Tian et al., 2017
MCM2_Fw_Hindlll primer (ACGATGAAGCTTATGGCGGAATCATCGGAATCCTTC)	IDT	N/A
MCM2_Rev_STOP_Xhol primer (AGCGGCCTCGAGATTATCAGAACTGCTGCAGGATCATTTTCC)	IDT	N/A

REAGENT or RESOURCE	SOURCE	IDENTIFIER
FANCM gRNA for CRISPR KO (TCAAGTATCTCCCGATCATC)	This paper	N/A
Recombinant DNA		
FLAG-FANCM Wt plasmid	Weidong Wang Lab	Meetei et al., 2005
FLAG-FANCM K117R plasmid	Weidong Wang Lab	Meetei et al., 2005
FLAG-FANCM Wt plasmid	Weidong Wang Lab	Singh et al., 2013
FLAG-FANCM S1045A mutant plasmid	Weidong Wang Lab	Singh et al., 2013
GFP-FANCM S1045A plasmid	Weidong Wang Lab	N/A
FLAG-MCM2 Wt plasmid	This work	N/A
FLAG-MCM2 S108A plasmid	This work	N/A
pCMV-(DYKDDDDK)-N vector	TakaraBio	Cat# 635688
Plasmid pDC690: pLPCX MCM2 Wt	David Cortez lab	Cortez et al., 2004
Plasmid pDC6914: pLPCX MCM2 S108A	David Cortez lab	Cortez et al., 2004
Software and Algorithms		
AxioVision SE64 Rel. 4.9.1	Zeiss	https://www.zeiss.com/microscopy/int/downloads.html
Image Lab software.	Bio-Rad	http://www.bio-rad.com
Volocity Version 6.3.0	Quorum Technologies	https://www.quorumtechnologies.com/
Sigmaplot 13.0	Systat Software Inc.	https://systatsoftware.com
Duolink Image Tool	Sigma-Aldrich	https://www.sigmaaldrich.com